Inventory of Supplemental Information

Supplemental Tables

Table S1, related to Figure 1.

Table S2, related to Figure 2.

Table S3, related to Figure 4.

Table S4, related to Figure 5.

Supplemental Figures

Figure S1, related to Figure 2.

Figure S2, related to Figure 3.

Figure S3, related to Figure 4.

Figure S4, related to Figure 4.

Figure S5, related to Figure 5.

Figure S6, related to Figure 6.

Figure S7, related to Figure 7.

Figure S8, related to Figure 7.

Figure S9, related to Figure 7.

Figure S10, rated to Figure 7.

Figure S11, related to Figure 8.

Supplemental Methods

Supplemental References

Supplemental Data

Table S1A*, related to figure 1*

Genotype distribution of *Brca1*$^{185stop/+}$ x *Brca1*$^{185stop/+}$ offspring

Genotype	All	+/+	185stop/+	185stop/ 185stop	n.d.
E7.5	17	4 (4.25)	13 (8.5)	0 (4.25)	0
E8.5	34	9 (8.5)	17 (17)	5 (8.5)	3
E9.5	10	2 (2.5)	6 (5)	2 (2.5)	0
E10.5	20	4 (5)	10 (10)	6 (5)	0
E11.5	17	6 (4.25)	7 (8.5)	1 (4.25)	3*
E13.5	40	11 (10)	23 (20)	2* (10)	4*
Postnatal	40	10 (10)	30 (20)	0 (10)	0

Table S1B*, related to figure 1*

Genotype distribution of *Brca1*$^{5382stop/+}$ x *Brca1*$^{5382stop/+}$ offspring

Genotype	All	+/+	5382stop/+	5382stop/ 5382stop	n.d.
E7.5	2	1 (0.5)	1 (1)	0 (0.5)	0
E8.5	31	7 (7.75)	17 (15.5)	7 (7.75)	0
E9.5	22	6 (5.5)	10 (11)	3 (5.5)	3
E12.5	23	4 (5.75)	13 (11.5)	1* (5.75)	5*
Postnatal	30	9 (7.5)	21 (15)	0 (7.5)	0

The expected number of mice according to Mendelian ratio is depicted between brackets. Resorbed embryos are depicted with *. Embryos of which the genotype could not be determined are displayed in the n.d. column.

Table S2*, related to figure 2*

Immunohistochemical characterization of *KB1(185stop)P* and *KB1(5382stop)P* mammary tumors

	Cytokeratin 8			Vimentin			ER		PR	
	+	+/-	-	+	+/-	-	+	-	+	-
KB1(185stop)P	87	4	9	17	4	78	13	87	22	78
KB1(5382stop)P	100	0	0	10	24	67	14	86	10	90

KB1(185stop)P (n=23) and *KB1(5382stop)P* (n=21) mammary tumors were scored positive (+), negative (-) or partly positive (+/-) for cytokeratin 8 and vimentin. Cytokeratin 8+/- = expression in mammary tubules and small tumor lobules, not in larger lobules. Vimentin +/- = some expression in non-solid parts of the tumor. Tumors were scored positive (+) for estrogen receptor (ER) or progesterone receptor (PR) when more than 10% of cells showed staining. Represented is the percentage of tumors.

Table S3A*, related to figure 4*

Overview transplanted *KB1(185stop)P* tumors

	Donor tumor				
# of tumors	**T1**	**T2**	**T3**	**T4**	**T5**
Transplanted	9	10	10	10	10
Outgrowth	3/9	10/10	9/10	10/10	10/10
No treatment	1/3	1/10	1/9	1/10	1/10
Cisplatin treatment	2/3	9/10	8/9	9/10	9/10
Cisplatin-resistant	2/2	3/9	5/8	6/9	7/9
Genetic reversion	0/2	0/3	0/5	0/6	0/7

Table S3B*, related to figure 4*

Overview transplanted *KB1(5382stop)P* tumors

	Donor tumor					
# of tumors	**T1**	**T2**	**T3**	**T4**	**T5**	**T6**
Transplanted	10	10	10	10	10	10
Outgrowth	8/10	9/10	10/10	10/10	6/10	10/10
No treatment	1/8	1/9	1/10	1/10	1/6	1/10
Cisplatin treatment	7/8	8/9	9/10	9/10	5/6	9/10
Cisplatin-resistant	0/7	1/8	1/9	0/9	0/5	0/9
Genetic reversion	0/0	0/0	0/0	0/0	0/0	0/0

T1 = spontaneous donor tumor 1, T2 = spontaneous donor tumor 2, T3 = spontaneous donor tumor 3, T4 = spontaneous donor tumor 4, T5 = spontaneous donor tumor 5 and T6 = spontaneous donor tumor 6.

Table S3C*, related to figure 4*

Average cisplatin IC_{50} values (IC_{50}av) human cancer cell lines

CELL LINE	IC_{50}av (µM)
U2OS	1,2096
HCC1937 + BRCA1	0,5753
HCC1937	0,2254
SUM149	0,1275
SUM1315	0,3055

Table S3D*, related to figure 4*

Statistical significance of differences in average cisplatin IC_{50} values (IC_{50}av) of human cancer cell lines (two-tailed t test)

CELL LINE	U2OS	HCC1937 + BRCA1	HCC1937	SUM149	SUM1315
U2OS		0,0026	0,0003	0,0001	0,0004
HCC1937 + BRCA1	0,0026		0,0001	0,0001	0,0001
HCC1937	0,0003	0,0001		0,0008	0,0055
SUM149	0,0001	0,0001	0,0008		0,0001
SUM1315	0,0004	0,0001	0,0055	0,0001	

Table S4*, related to figure 5*

Overview of BRCA1 mass spectrometry results for *KB1(185stop)P* mouse mammary tumor cell lines 288 and 350 and a mouse BRCA1 wild-type (WT) expressing control cell line

CELL LINE	Experiment number	Coverage BRCA1	Peptides RING/total	Most N-terminal amino acids
BRCA1-WT	MS1240	63%	11/214	21-32
BRCA1-WT	MS1280	50%	12/316	21-32
BRCA1-WT	MS1292	7%	3/19	79-88
BRCA1-185stop 288	MS1240	37%	0/91	118-131
BRCA1-185stop 288	MS1280	23%	0/82	118-131
BRCA1-185stop 288	MS1292	14%	0/43	118-131
BRCA1-185stop 350	MS1240	61%	0/199	118-131
BRCA1-185stop 350	MS1280	30%	0/88	118-131
BRCA1-185stop 350	MS1292	24%	0/63	118-131

Figure S1A-D

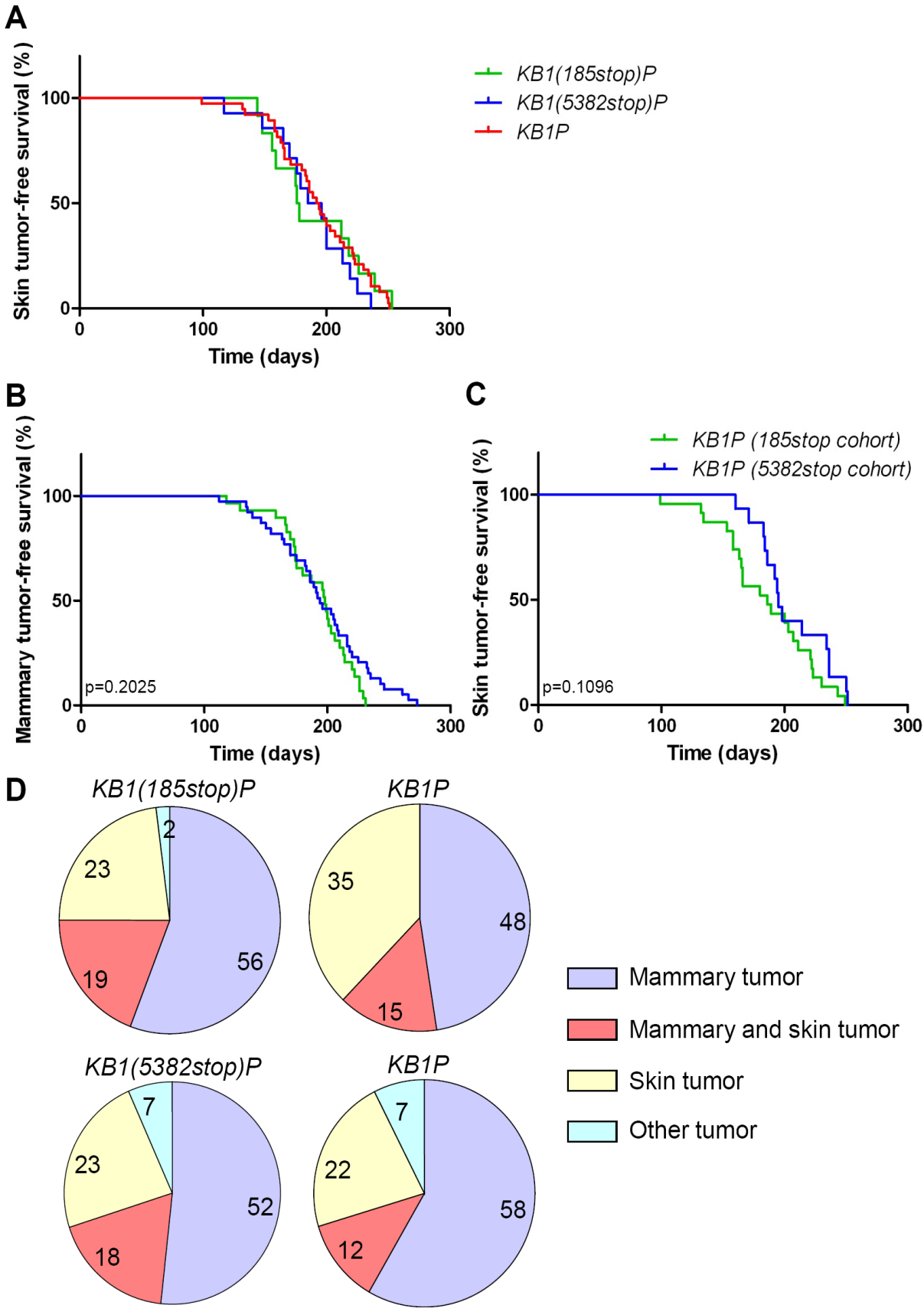
A
Skin tumor-free survival (%)
100
50
0
0
100
200
300
Time (days)
KB1(185stop)P
KB1(5382stop)P
KB1P
B
Mammary tumor-free survival (%)
p=0.2025
Time (days)
C
Skin tumor-free survival (%)
KB1P (185stop cohort)
KB1P (5382stop cohort)
p=0.1096
Time (days)
D
KB1(185stop)P
2
23
19
56
KB1P
35
48
15
KB1(5382stop)P
7
23
18
52
KB1P
7
22
12
58
Mammary tumor
Mammary and skin tumor
Skin tumor
Other tumor

Figure S1E-G

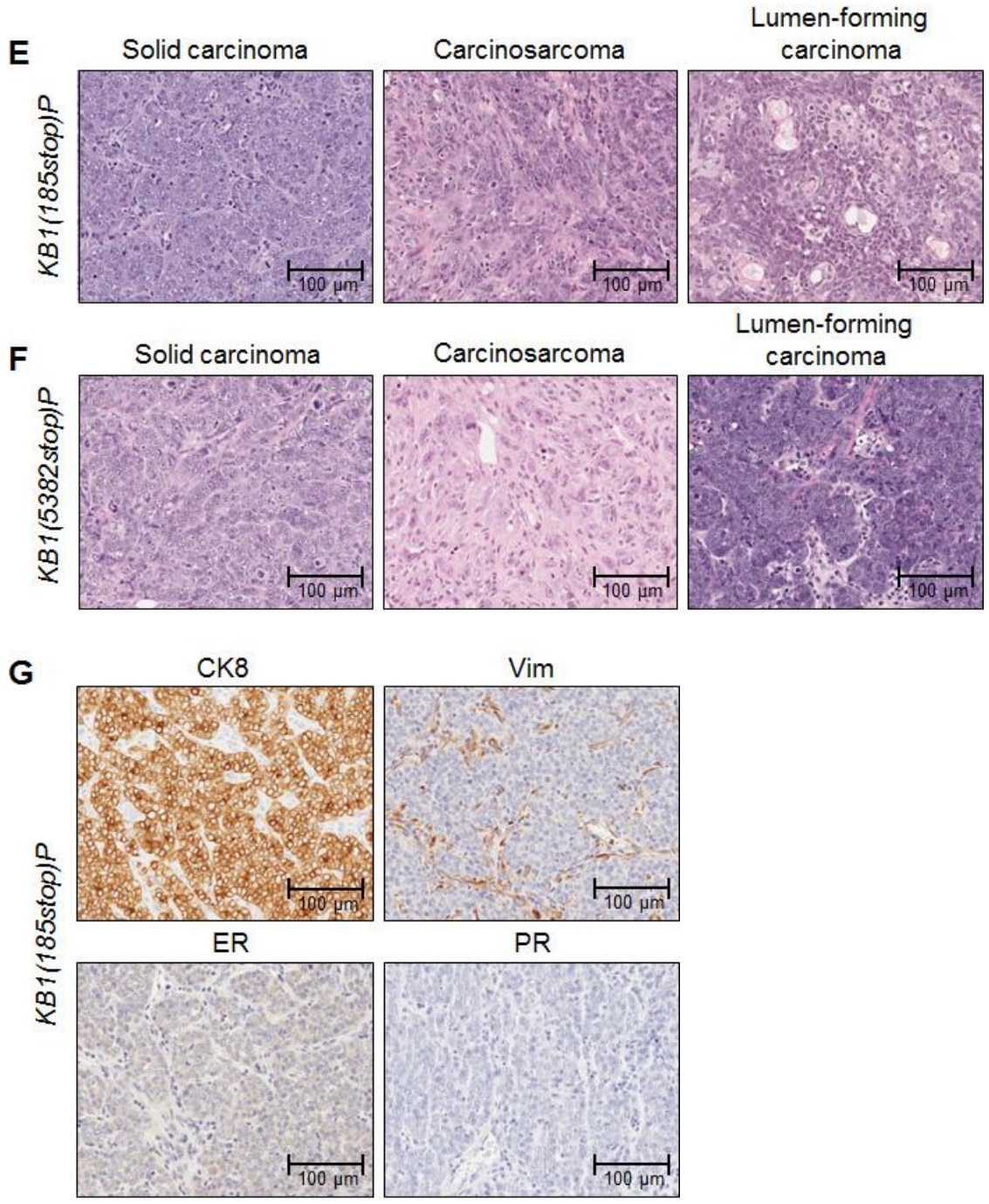
E
Solid carcinoma
Carcinosarcoma
Lumen-forming carcinoma
KB1(185stop)P
100 µm
F
Solid carcinoma
Carcinosarcoma
Lumen-forming carcinoma
KB1(5382stop)P
100 µm
G
CK8
Vim
ER
PR
KB1(185stop)P
100 µm

Figure S1H

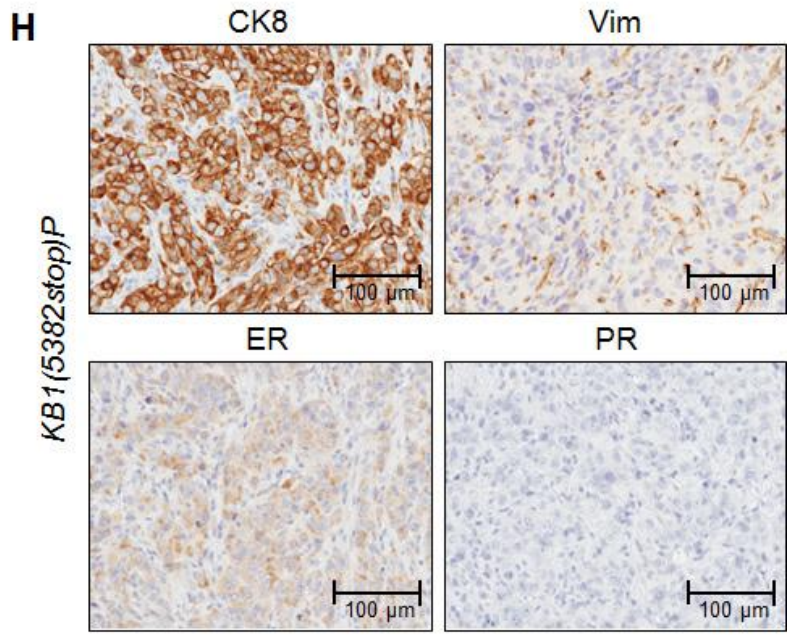

Figure S1, related to figure 2

Spontaneous tumor development in *KB1(185stop)P* and *KB1(5382stop)P* mice. (A) Skin tumor-free survival of *KB1(185stop)P* (green; T_{50}=177 days, n=12 mice) and *KB1(5382stop)P* mice (blue; T_{50}=191 days, n=14 mice). *KB1(185stop)P* vs. *KB1(5382stop)P* log-rank test p=0.5456. T_{50}: median survival, n: the number of mice. (B) Mammary tumor-free survival of *KB1P* mice from the *185stop* cohort (green; T_{50}=198 days, n=29 mice) and *KB1P* mice from the *5382stop* cohort (blue; T_{50}=194 days, n=39 mice). *KB1P (185stop* cohort*)* vs. *KB1P* (*5382stop* cohort) log-rank test p=0.2025. (C) Skin tumor-free survival of *KB1P* mice from the *185stop* cohort (green; T_{50}=186 days, n=23 mice) and *KB1P* mice from the *5382stop* cohort (blue; T_{50}=195 days, n=15 mice). *KB1(5382stop)P* vs. *KB1P* log-rank test p=0.1096. (D) Distribution in percentages of different tumor types in *KB1(185stop)P*, *KB1(5382stop)P* and *KB1P* mice. Purple: only one or multiple mammary tumor(s); orange: both mammary and skin tumor(s); yellow: only one or multiple skin tumor(s); blue: another kind of tumor. (E) HE pictures of different types of *KB1(185stop)P* mammary tumors. Scale bar represents 100 µm. (F) HE pictures of different types of *KB1(5382stop)P* mammary tumors. (G) Immunohistochemical characterization of *KB1(185stop)P* solid mammary carcinoma. CK8= cytokeratin 8, Vim= vimentin, ER= estrogen receptor, PR= progesterone receptor. Scale bar represents 100 µm. (H) Immunohistochemical characterization of *KB1(5382stop)P* solid mammary carcinoma.

Figure S2

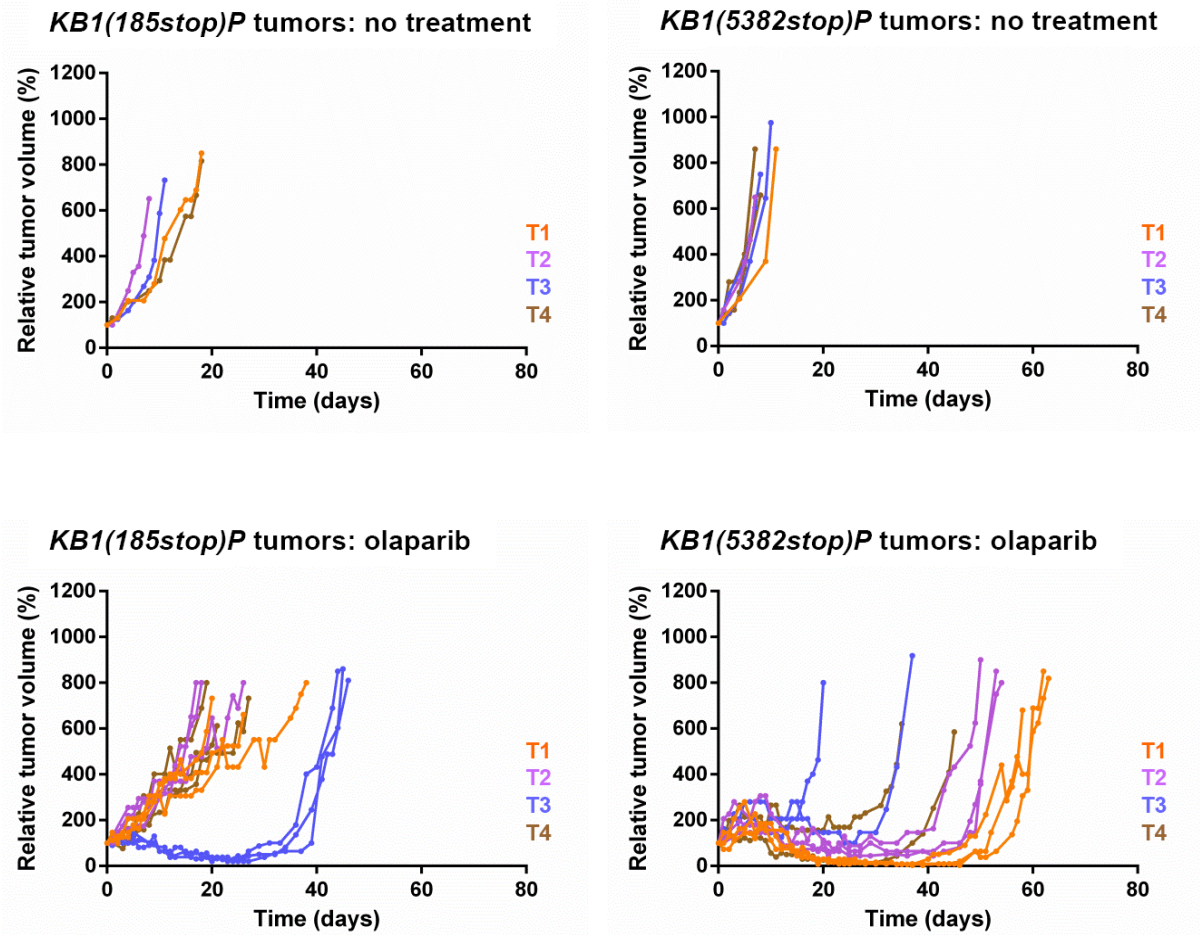

Figure S2, related to figure 3

Olaparib response of *KB1(185stop)P* and *KB1(5382stop)P* mammary tumors. Pieces of *KB1(185stop)P* and *KB1(5382stop)P* mouse mammary tumors were orthotopically transplanted into the fourth right mammary fat pad of syngeneic wild-type (FVB/n x 129/Ola) F1 female mice. When tumors reached a volume of 200 mm^3 (100%), mice were treated with 50 mg/kg olaparib for 28 consecutive days (lower panels) or left untreated (upper panels). Different colors represent individual spontaneous donor tumors, four from each strain.

Figure S3A-C

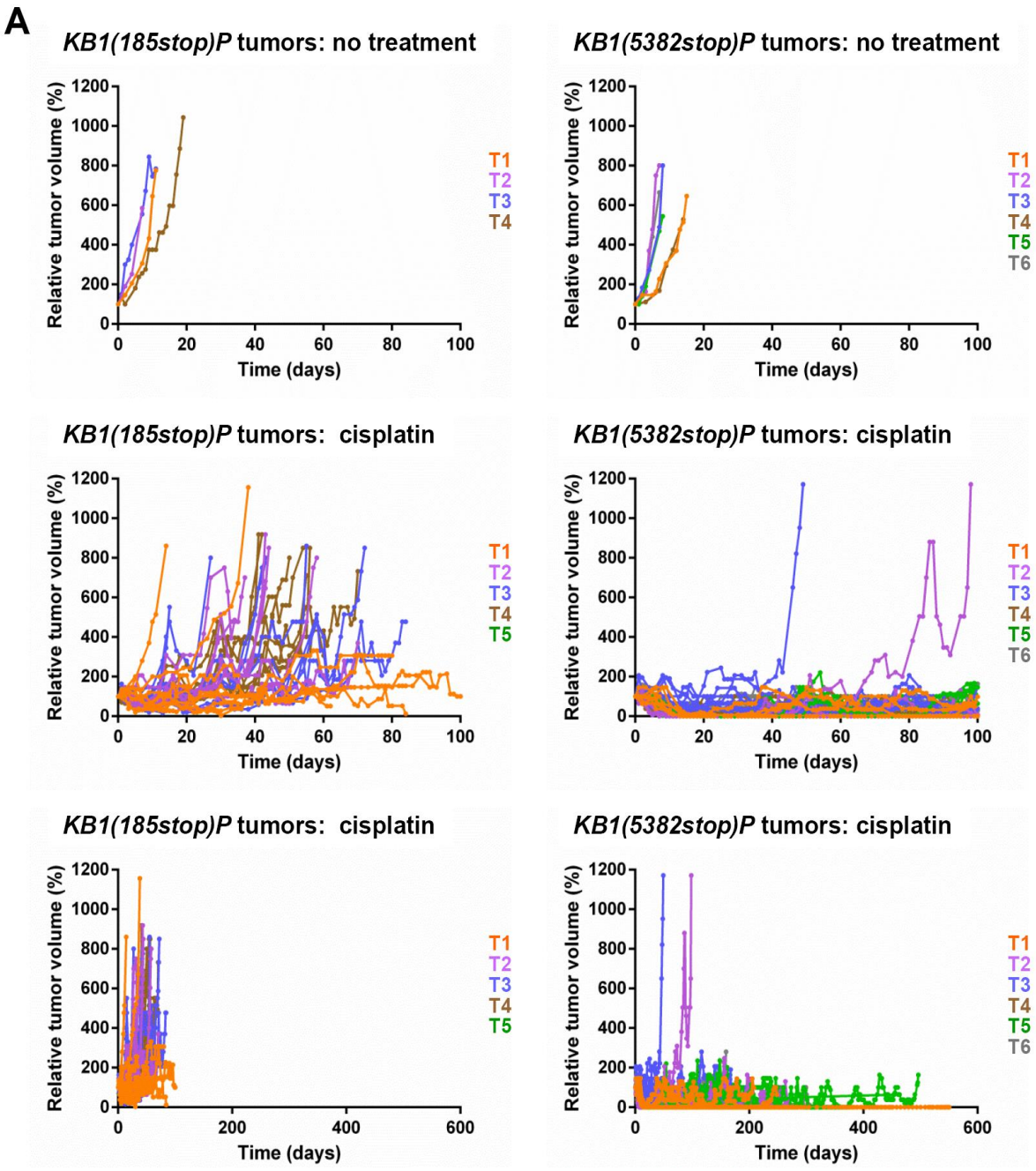
A
KB1(185stop)P tumors: no treatment
KB1(5382stop)P tumors: no treatment
KB1(185stop)P tumors: cisplatin
KB1(5382stop)P tumors: cisplatin
KB1(185stop)P tumors: cisplatin
KB1(5382stop)P tumors: cisplatin
Relative tumor volume (%)
Time (days)
T1
T2
T3
T4
T5
T6
B
KB1(185stop)P tumors: cisplatin
Overall survival (%)
Time (days)
C
KB1(5382stop)P tumors: cisplatin
Overall survival (%)
Time (days)

Figure S3D-F

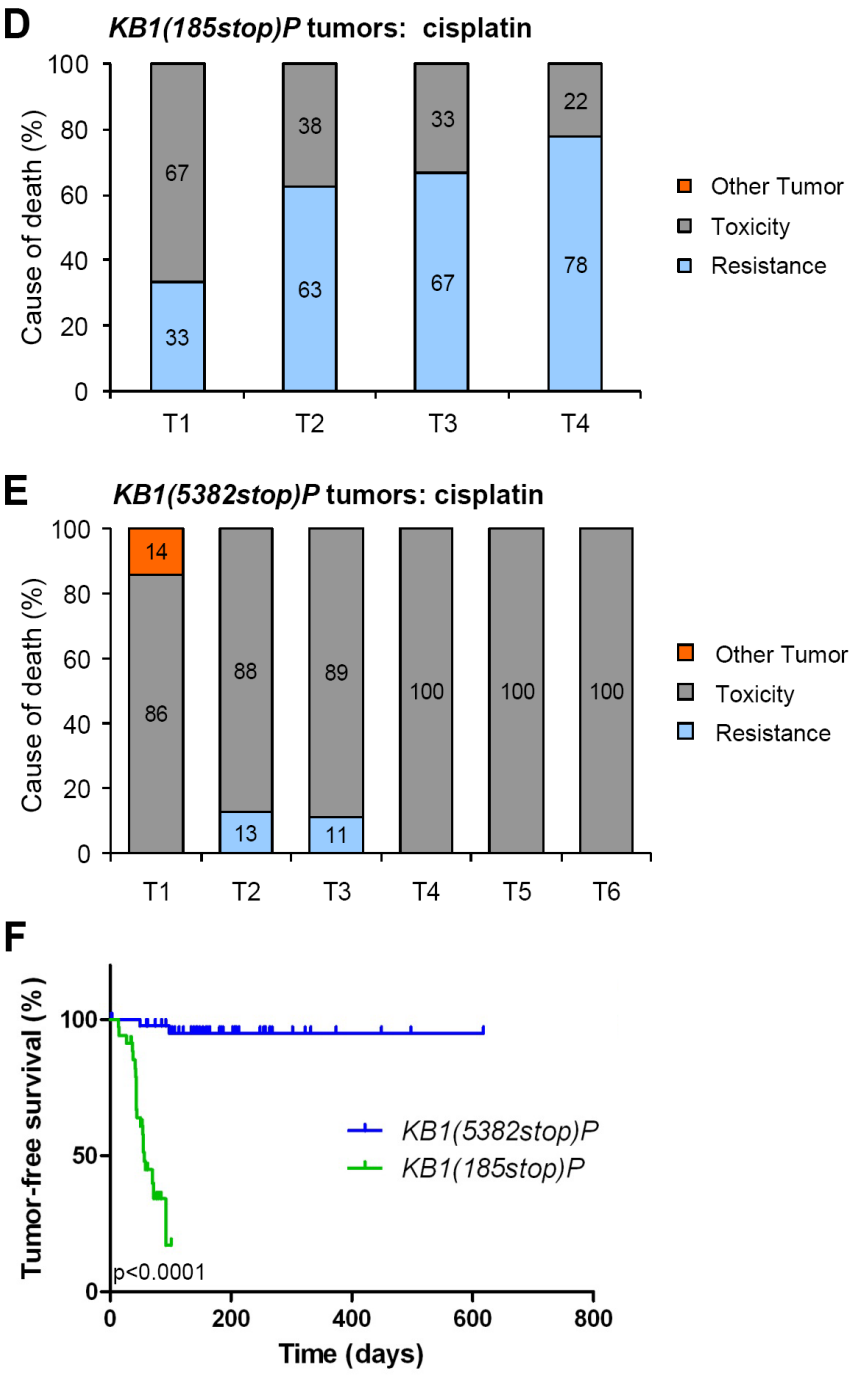

Figure S3, related to figure 4

Cisplatin response of *KB1(185stop)P* and *KB1(5382stop)P* mammary tumors. (A) Response to cisplatin treatment of individual mice transplanted with different *KB1(185stop)P* and *KB1(5382stop)P* mammary tumors. When tumors reached a volume of 200 mm^3 (100%), mice were injected intravenously with 6 mg/kg cisplatin and retreated every two weeks when the tumor volume was over 50% of the starting volume. If the tumor size after two weeks was smaller than 50%, treatment was postponed until the tumor reached 100% of the starting volume. Different colors represent individual spontaneous donor tumors. (B) OS of mice transplanted with *KB1(185stop)P* mammary tumors after cisplatin treatment (grouped per donor tumor). The blue line represents OS of mice transplanted with donor tumor 1 (T1; T_{50}= 62 days, n=9), the pink line

represents OS of mice transplanted with donor tumor 2 (T2; T_{50}=44 days, n=8), the yellow line represents OS of mice transplanted with donor tumor 3 (T3; T_{50}=55 days, n=9) and the green line represents OS of mice transplanted with donor tumor 4 (T4; T_{50}=54 days, n=9). T_{50}: median OS, n: the number of mice. (C) OS of mice transplanted with *KB1(5382stop)P* mammary tumors after cisplatin treatment (grouped per donor tumor). The blue line represents OS of mice transplanted with donor tumor 1 (T1; T_{50}=248 days, n=6), the pink line represents OS of mice transplanted with donor tumor 2 (T2; T_{50}=132 days, n=8), the yellow line represents OS of mice transplanted with donor tumor 3 (T3; T_{50}=92 days, n=9), the green line represents OS of mice transplanted with donor tumor 4 (T4; T_{50}=254 days, n=9), the purple line represents OS of mice transplanted with donor tumor 5 (T5; T_{50}=121 days, n=5) and the brown line represents OS of mice transplanted with donor tumor 6 (T6; T_{50}=154 days, n=9). (D) Causes of death of mice transplanted with *KB1(185stop)P* mammary tumors after cisplatin treatment (grouped per donor tumor). Mice that had to be sacrificed because of cisplatin-resistant mammary tumors are depicted in blue, mice that had to be sacrificed because of cisplatin-toxicity are depicted in grey and mice that died because of another type of tumor are depicted in orange. Percentages are indicated within the stacked bars. (E) Causes of death of mice transplanted with *KB1(5382stop)P* mammary tumors after cisplatin treatment (grouped per donor tumor). (F) Tumor-free survival of mice transplanted with *KB1(185stop)P* (green; T_{50}=56 days, n=35 mice) or *KB1(5382stop)P* mammary tumors (blue; T_{50}=undefined, n=47 mice) after cisplatin treatment. *KB1(185stop)P* vs. *KB1(5382stop)P* log-rank test $p<0.0001$.

Figure S4A-C

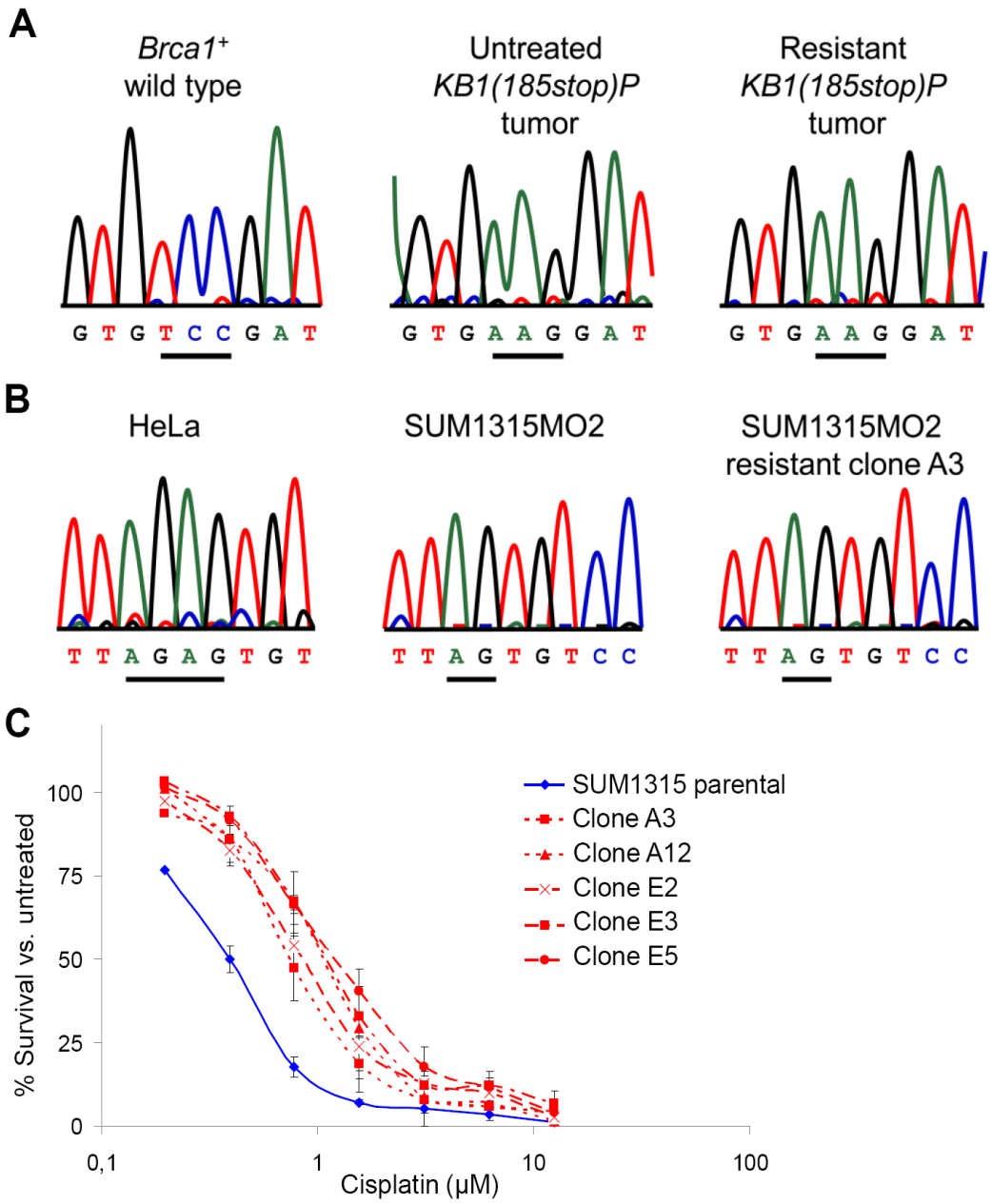
A
Brca1+
wild type
Untreated
KB1(185stop)P
tumor
Resistant
KB1(185stop)P
tumor
G T G T C C G A T
G T G A A G G A T
G T G A A G G A T
B
HeLa
SUM1315MO2
SUM1315MO2
resistant clone A3
T T A G A G T G T
T T A G T G T C C
T T A G T G T C C
C
% Survival vs. untreated
100
75
50
25
0
0,1
1
10
100
Cisplatin (μM)
SUM1315 parental
Clone A3
Clone A12
Clone E2
Clone E3
Clone E5

Figure S4D-E

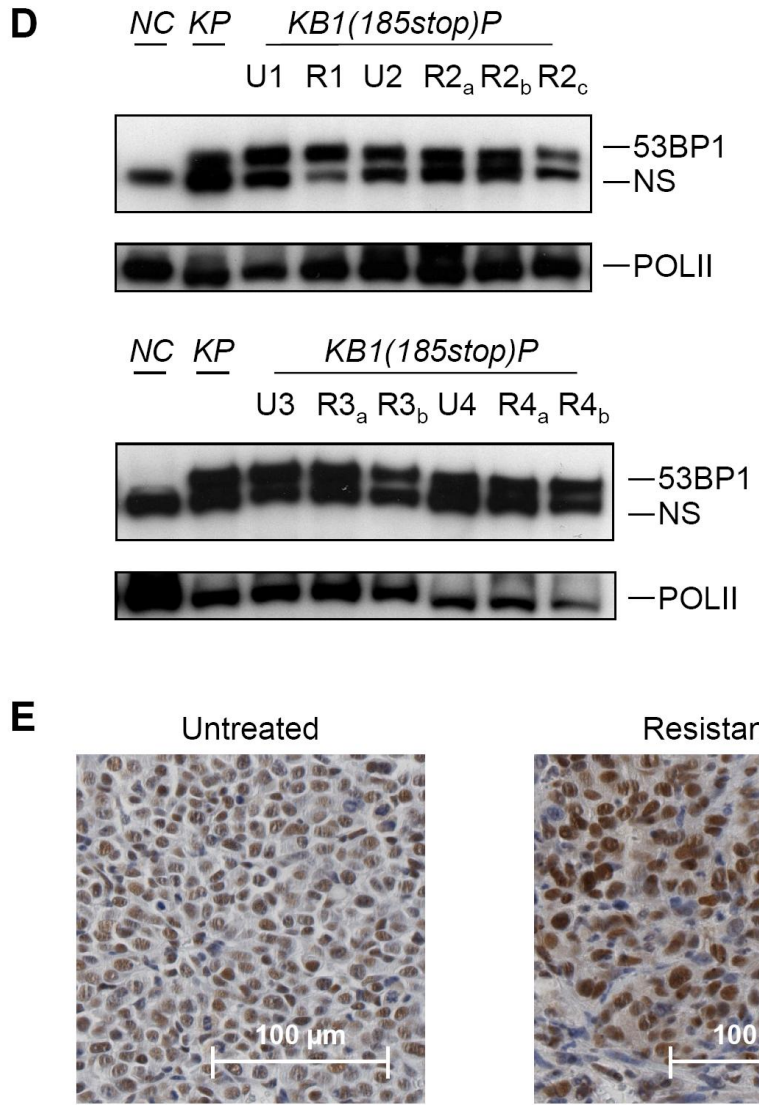

Figure S4, related to figure 5

Platinum resistant *KB1(185stop)P* tumors or SUM1315MO2 cells do not show genetic reversion of BRCA1 or loss of 53BP1. (A) Sequencing plots of *KB1(185stop)P* tumor DNA showing that 3 nt substitution in the *Brca1*^{185stop} allele (TCC>AAG) is retained in cisplatin-resistant mouse mammary tumors. (B) Sequencing plots of DNA derived from HeLa cells, SUM1315MO2 parental cells and clone A3, indicating that the *BRCA1*^{185delAG} mutation is retained in cisplatin-resistant SUM1315MO2 clones. (C) Cisplatin sensitivity of SUM1315MO2 parental cells (blue curve) and cisplatin-selected SUM1315MO2 clones A3, A12, E2, E3 and E5 (red curves). The experiment was performed in triplicate. Error bars indicate SEM. (D) 53BP1 protein expression in tumors derived from four different donor tumors (1-4). Of each donor tumor, untreated (U1-U4) and platinum-resistant *KB1(185stop)P* mouse mammary tumors (R1-R4) are shown. Each lane contains separately transplanted tumors. 53BP1 expression in a BRCA1-proficient *KP* tumor was used as positive control and a 53BP1 negative ES clone was used as a negative control (NC). Expression of POLII was used as loading control. (E) Examples of 53BP1 immunohistochemistry on *KB1(185stop)P* mouse mammary tumors. All non-treated (n=5) and platinum-resistant (n=23) tumors showed abundant nuclear staining for 53BP1.

Figure S5A

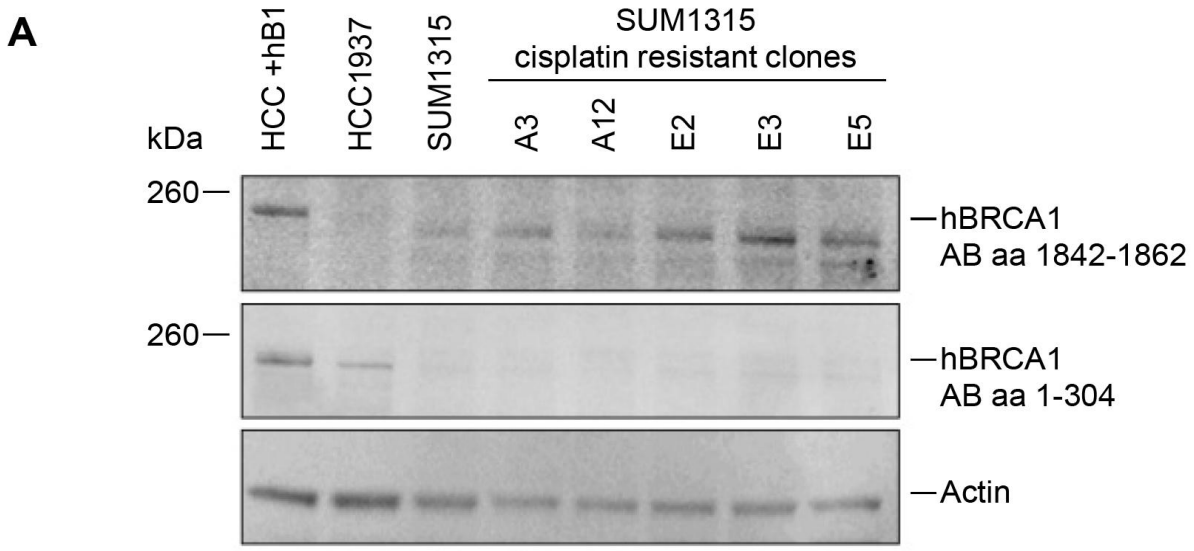
A
HCC +hB1
HCC1937
SUM1315
SUM1315
cisplatin resistant clones
A3
A12
E2
E3
E5
kDa
260
260
hBRCA1
AB aa 1842-1862
hBRCA1
AB aa 1-304
Actin

Figure S5B

B

Brca1 wild-type tumor cells

```
   1 MDLSAVQIQE VQNVLHAMQK ILECPICLEL IKEPVSTKCD HIFCKFCMLK
  51 LLNQKKGPSQ CPLCKNEITK RSLQGSTRFS QLAEELLRIM AAFELDTGMQ
 101 LTNGFSFSKK RNNSCERLNE EASIIQSVGY RNRVRRLPQV EPGNATLKDS
 151 LGVQLSNLGI VRSVKKNRQT QPRKKSVYIE LDSDSSEETV TKPGDCSVRD
 201 QELLQTAPQE AGDEGKLHSA EEAACEFSEG IRNIEHHQCS DDLNPTENHA
 251 TERHPEKCQS ISISNVCVEP CGTDAHASSL QPETSSLLLI EDRMNAEKAE
 301 FCNKSKQPGI AVSQQSRWAA SKGTCNDRQV PSTGEKVGPN ADSLSDREKW
 351 THPQSLCPEN SGATTDVPWI TLNSSVQKVN EWFSRTGEML TSDSASARRH
 401 ESNAEAAVVL EVSNEVDGGF SSSRKTDLVT PDPHHTLMCK SGRDFSKPVE
 451 DNISDKIFGK SYQRKGSRPH LNHVTEIIGT FITEPQITQE QPFTNKLKRK
 501 RSTSLQPEDF IKKADSAGVQ RTPDNINQGT DLMEPNEQAV STTSNCQENK
 551 IAGSNLQKEK SAHPTESLRK EPASTAGAKS ISNSVSDLEV ELNVHSSKAP
 601 KKNRLRRKSS IRCALPLEPI SRNPSPPTCA ELQIDSCGSS EETKKNHSNQ
 651 QPAGHLREPQ LIEDTEPAAD AKKNEPNEHI RKRRASDAFP EEKLMNKAGL
 701 LTSCSSPRKS QGPVNPSPQR TGTEQLETRQ MSDSAKELGD RVLGGEPSGK
 751 TTDRSEESTS VSLVSDTDYD TQNSVSVLDA HTVRYARTGS AQCMTQFVAS
 801 ENPKELVHGS NNAGSGTEGL KPPLRHALNL SQEKVEMEDS ELDTQYLQNT
 851 FQVSKRQSFA LFSKPRSPQK DCAHSVPSKE LSPKVTAKGK QKERQGQEEF
 901 EISHVQAVAA TVGLPVPCQE GKLAADTMCD RGCRLCPSSH YRSGENGLSA
 951 TGKSGISQNS HFKQSVSPIR SSIKTDNRKP LTEGRFERHT SSTEMAVGNE
1001 NILQSTVHTV SLNNRGNACQ EAGSGSIHEV CSTGDSFPGQ LGRNRGPKVN
1051 TVPPLDSMQP GVCQQSVPVS DKYLEIKKQE GEAVCADFSP CLFSDHLEQS
1101 MSGKVFQVCS ETPDDLLDDV EIQGHTSFGE GDIMERSAVF NGSILRRESS
1151 RSPSPVTHAS KSQSLHRASR KLESSEESDS TEDEDLPCFQ HLLSRISNTP
1201 ELTRCSSAVT QRMPEKAEGT QAPWKGSSSD CNNEVIMIEA SQEHQFSEDP
1251 RCSGSMFSSQ HSAAQGSTAN ANSQDSNFIP PSKQRSHQCG NEEAFLSDKE
1301 LISDNEEMAT CLEEDNDQEE DSIIPDSEAS GYESETNLSE DCSQSDILTT
1351 QQRATMKYNL IKLQQEMAHL EAVLEQRGNQ PSGHSPSLLA DPCALEDLPD
1401 LEPNMSGAAI LTSKNINENP VSQNLKSACD DKFQLQHLEG PTSGDDESGM
1451 GRPSPFKSPL AGSRGSAHGC SRHLQKRNSP SQEELLQPAG SEASSEPHNS
1501 TGQSCLPRRE LEGTPYLGSG ISLFSSRDPE SESPKEPAHI GTTPASTSAL
1551 KIPQGQVAFR SAAAAGADKA VVGIVSKIKP ELTSSEERAD RDISMVVSGL
1601 TPKEVMTVQK FAEKYRLTLT DAITEETTHV IIKTDAEFVC ERTLKYFLGI
1651 AGGKWIVSYS WVVRSIQERR LLNVHEFEVK GDVVTGRNHQ GPRRSRESRE
1701 KLFKGLQVYC CEPFTNMPKD ELERMLQLCG ASVVKELPSL THDTGAHLVV
1751 IVQPSAWTED SNCPDIGQLC KARLVMWDWV LDSLSSYRCR DLDAYLVQNI
1801 TCDSSEPQDS ND
```

KB1(185stop)P tumor cells

```
   1 MDLSAVQIQE VQNVLHAMQK ILECPICLEL IKEPVSTKCD HIFCKFCMLK
  51 LLNQKKGPSQ CPLCKNEITK RSLQGSTRFS QLAEELLRIM AAFELDTGMQ
 101 LTNGFSFSKK RNNSCERLNE EASIIQSVGY RNRVRRLPQV EPGNATLKDS
 151 LGVQLSNLGI VRSVKKNRQT QPRKKSVYIE LDSDSSEETV TKPGDCSVRD
 201 QELLQTAPQE AGDEGKLHSA EEAACEFSEG IRNIEHHQCS DDLNPTENHA
 251 TERHPEKCQS ISISNVCVEP CGTDAHASSL QPETSSLLLI EDRMNAEKAE
 301 FCNKSKQPGI AVSQQSRWAA SKGTCNDRQV PSTGEKVGPN ADSLSDREKW
 351 THPQSLCPEN SGATTDVPWI TLNSSVQKVN EWFSRTGEML TSDSASARRH
 401 ESNAEAAVVL EVSNEVDGGF SSSRKTDLVT PDPHHTLMCK SGRDFSKPVE
 451 DNISDKIFGK SYQRKGSRPH LNHVTEIIGT FITEPQITQE QPFTNKLKRK
 501 RSTSLQPEDF IKKADSAGVQ RTPDNINQGT DLMEPNEQAV STTSNCQENK
 551 IAGSNLQKEK SAHPTESLRK EPASTAGAKS ISNSVSDLEV ELNVHSSKAP
 601 KKNRLRRKSS IRCALPLEPI SRNPSPPTCA ELQIDSCGSS EETKKNHSNQ
 651 QPAGHLREPQ LIEDTEPAAD AKKNEPNEHI RKRRASDAFP EEKLMNKAGL
 701 LTSCSSPRKS QGPVNPSPQR TGTEQLETRQ MSDSAKELGD RVLGGEPSGK
 751 TTDRSEESTS VSLVSDTDYD TQNSVSVLDA HTVRYARTGS AQCMTQFVAS
 801 ENPKELVHGS NNAGSGTEGL KPPLRHALNL SQEKVEMEDS ELDTQYLQNT
 851 FQVSKRQSFA LFSKPRSPQK DCAHSVPSKE LSPKVTAKGK QKERQGQEEF
 901 EISHVQAVAA TVGLPVPCQE GKLAADTMCD RGCRLCPSSH YRSGENGLSA
 951 TGKSGISQNS HFKQSVSPIR SSIKTDNRKP LTEGRFERHT SSTEMAVGNE
1001 NILQSTVHTV SLNNRGNACQ EAGSGSIHEV CSTGDSFPGQ LGRNRGPKVN
1051 TVPPLDSMQP GVCQQSVPVS DKYLEIKKQE GEAVCADFSP CLFSDHLEQS
1101 MSGKVFQVCS ETPDDLLDDV EIQGHTSFGE GDIMERSAVF NGSILRRESS
1151 RSPSPVTHAS KSQSLHRASR KLESSEESDS TEDEDLPCFQ HLLSRISNTP
1201 ELTRCSSAVT QRMPEKAEGT QAPWKGSSSD CNNEVIMIEA SQEHQFSEDP
1251 RCSGSMFSSQ HSAAQGSTAN ANSQDSNFIP PSKQRSHQCG NEEAFLSDKE
1301 LISDNEEMAT CLEEDNDQEE DSIIPDSEAS GYESETNLSE DCSQSDILTT
1351 QQRATMKYNL IKLQQEMAHL EAVLEQRGNQ PSGHSPSLLA DPCALEDLPD
1401 LEPNMSGAAI LTSKNINENP VSQNLKSACD DKFQLQHLEG PTSGDDESGM
1451 GRPSPFKSPL AGSRGSAHGC SRHLQKRNSP SQEELLQPAG SEASSEPHNS
1501 TGQSCLPRRE LEGTPYLGSG ISLFSSRDPE SESPKEPAHI GTTPASTSAL
1551 KIPQGQVAFR SAAAAGADKA VVGIVSKIKP ELTSSEERAD RDISMVVSGL
1601 TPKEVMTVQK FAEKYRLTLT DAITEETTHV IIKTDAEFVC ERTLKYFLGI
1651 AGGKWIVSYS WVVRSIQERR LLNVHEFEVK GDVVTGRNHQ GPRRSRESRE
1701 KLFKGLQVYC CEPFTNMPKD ELERMLQLCG ASVVKELPSL THDTGAHLVV
1751 IVQPSAWTED SNCPDIGQLC KARLVMWDWV LDSLSSYRCR DLDAYLVQNI
1801 TCDSSEPQDS ND
```

Full-length mouse BRCA1 amino acids. Red: BRCA1 peptides identified by mass spectrometry in *Brca1* wild-type and *KB1(185stop)P* mouse mammary tumor cells. Green: putative translation start site. Boxed: RING domain (aa 1-109).

Figure S5C-D

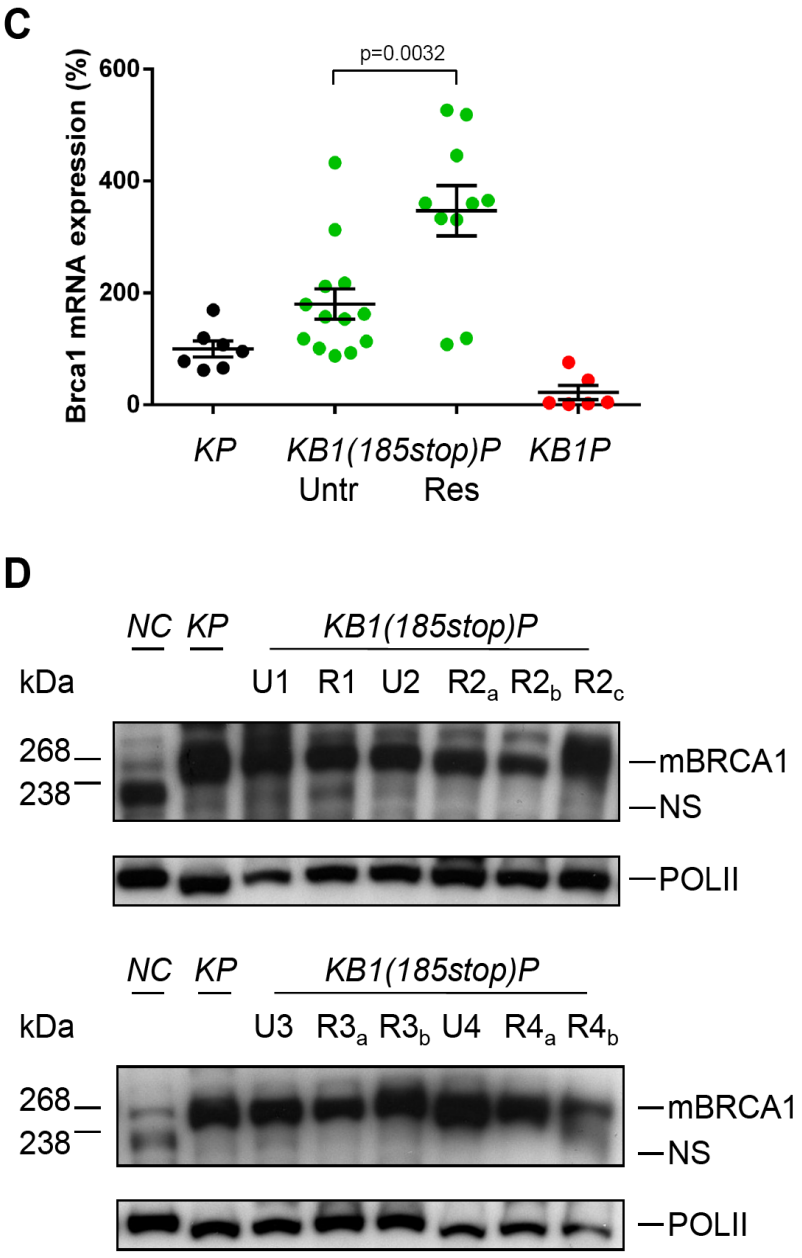
C
p=0.0032
Brca1 mRNA expression (%)
600
400
200
0
KP
KB1(185stop)P
Untr
KB1(185stop)P
Res
KB1P
D
NC
KP
KB1(185stop)P
kDa
U1
R1
U2
R2a
R2b
R2c
268
238
mBRCA1
NS
POLII
NC
KP
KB1(185stop)P
kDa
U3
R3a
R3b
U4
R4a
R4b
268
238
mBRCA1
NS
POLII

Figure S5, related to figure 5

BRCA1 expression in platinum-resistant mouse *Brca1*^{185stop} and *Brca1*^{53825stop} tumors and cisplatin-selected SUM1315MO2 clones.

(A) BRCA1 protein expression in human breast cancer cell lines HCC1937, SUM1315MO2 and cisplatin-resistant clones of SUM1315MO2 (A3, A12, E2, E3 and E5). The HCC1937 cell line serves as a negative control. The HCC1937 cell line complemented with human BRCA1 was used as positive control. Expression of Actin was used as loading control. (B) Amino acid composition of mouse BRCA1 for *Brca1* wild-type and *KB1(185stop)P* mouse mammary tumor cell lines. Peptides identified by mass spectrometry are indicated in red. Putative translation start sites are marked green (M1 for Brca1 wild-type cells and M90 for *KB1(185stop)P* cells). (C) *Brca1* mRNA expression in *KP* (black), untreated and platinum-resistant *KB1(185stop)P* (green), and *KB1P* (red) mouse mammary tumors. The average *Brca1* mRNA expression in several BRCA1-proficient *KP* tumors was used for normalization. *KB1(185stop)P* untreated vs. *KB1(185stop)P* resistant unpaired two-tailed t test p=0.0032. Error bars indicate SEM. (D) BRCA1 protein expression in *KB1(185stop)P* mouse mammary tumors derived from four different donor tumors (1-4). Of each donor tumor, untreated (U1-U4) and platinum-resistant tumors (R1-R4) are shown. Each lane contains separately transplanted tumors. BRCA1 expression in a BRCA1-proficient *KP* tumor was used as positive control and a BRCA1 negative ES clone was used as a negative control (NC). Expression of POLII was used as loading control.

Figure S6A-B

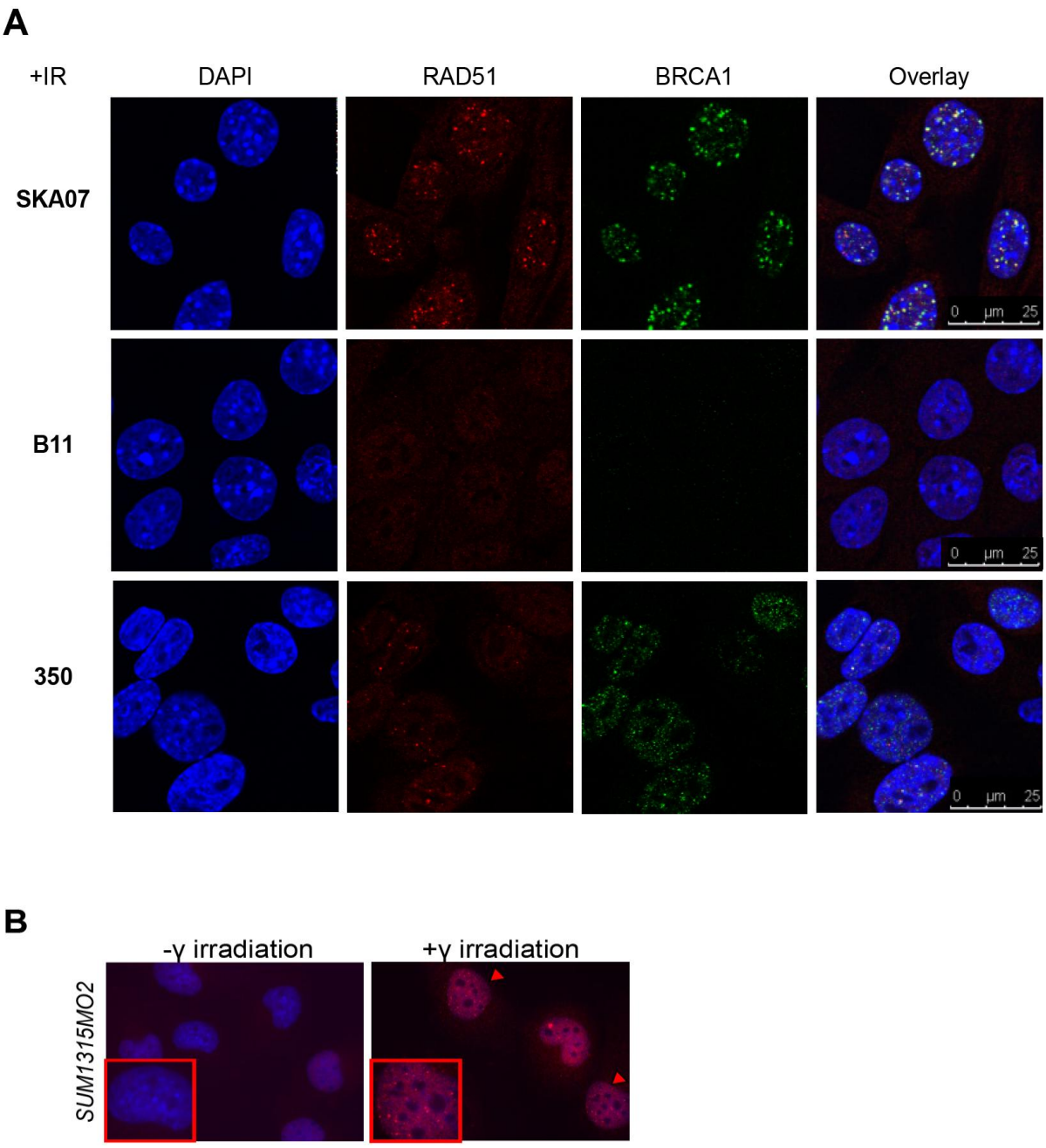

Figure S6, related to figure 6
DNA damage response of *Brca1*^{185stop} mouse tumor cell lines and *BRCA1*^{185delAG} human tumor cells. (A) Immunofluorescence of RAD51 (red) and BRCA1 (green) foci after treatment with gamma irradiation (10Gy) of BRCA1-proficient SKA07, BRCA1-deficient B11 and *Brca1*^{185stop} 350 mouse mammary tumor cells. Nuclei were visualized with DAPI (blue; left panel). Yellow dots in the overlay pictures (right panel) represent BRCA1/RAD51 colocalization. Scale bars are indicated on the overlay pictures. (B) Immunofluorescence of RAD51 foci in human SUM1315MO2 breast cancer cells with or without gamma irradiation (10Gy). Cells with more than 10 RAD51 foci (red) are indicated with red arrowheads. Red square: single cell zoom-in. Nuclei were visualized with DAPI (blue). All pictures were taken at a 63x magnification.

Figure S7A-C

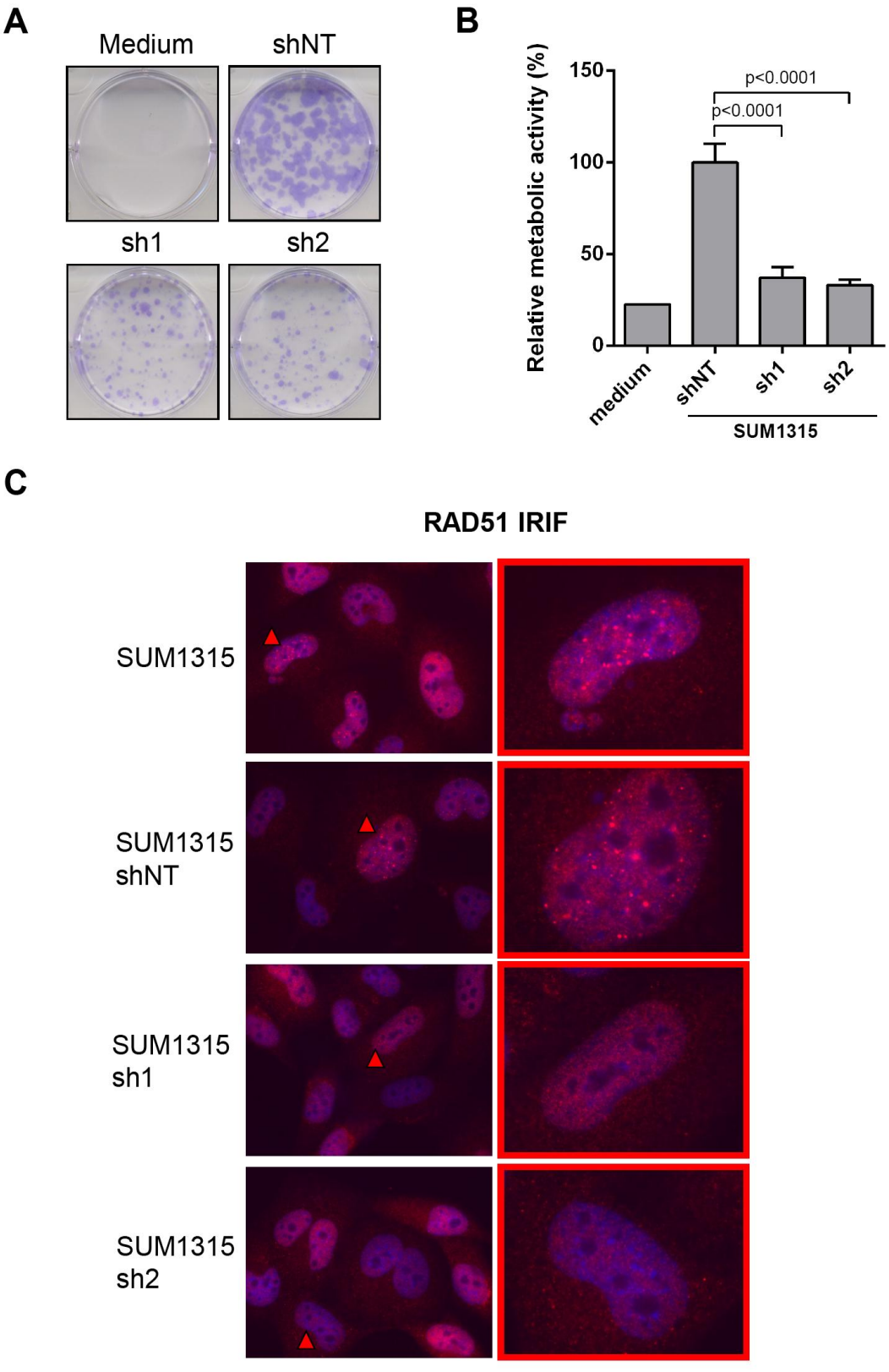
A
Medium
shNT
sh1
sh2
B
Relative metabolic activity (%)
150
100
50
0
p<0.0001
p<0.0001
medium
shNT
sh1
sh2
SUM1315
C
RAD51 IRIF
SUM1315
SUM1315
shNT
SUM1315
sh1
SUM1315
sh2

Figure S7D-F

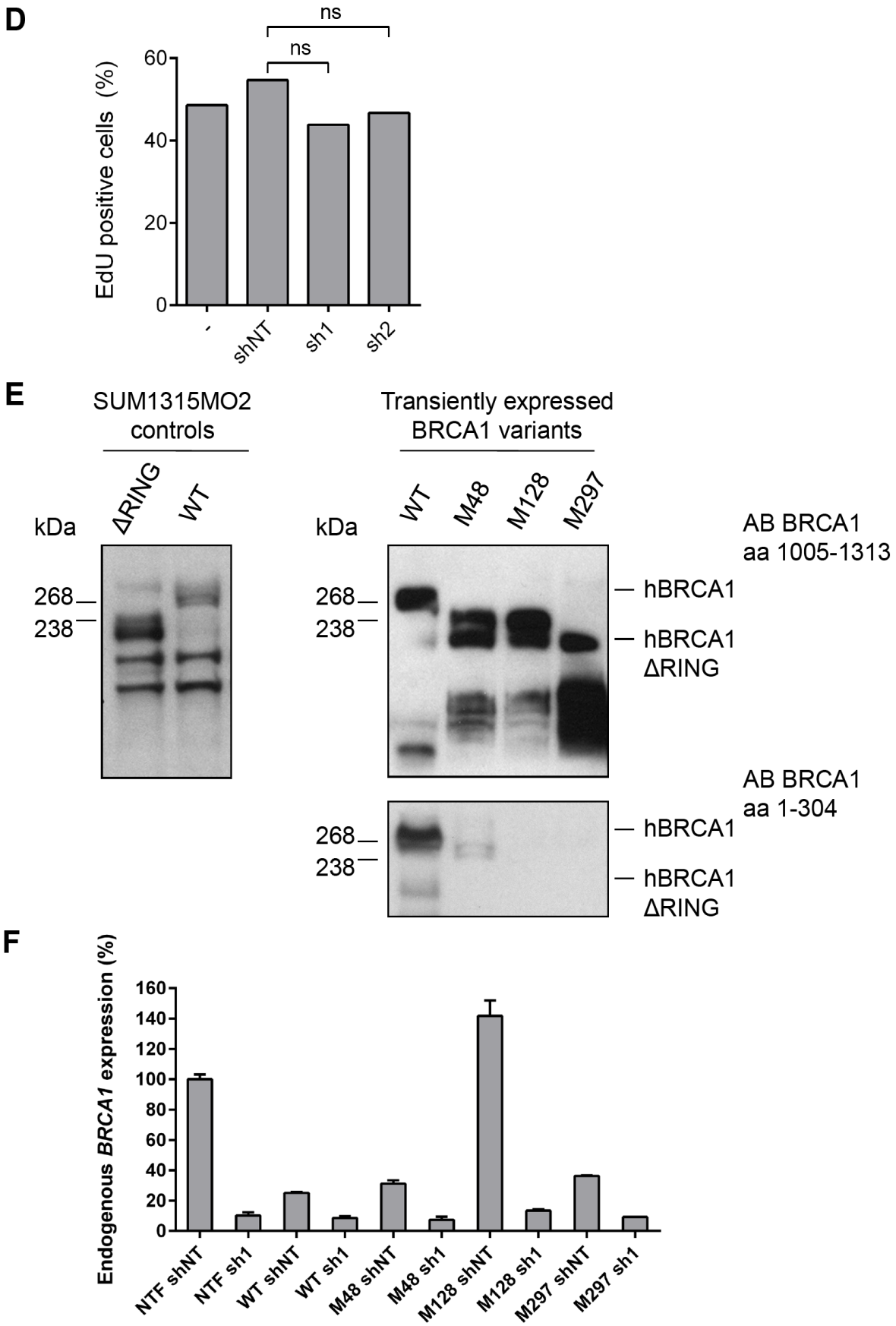
D
ns
ns
60
40
20
0
EdU positive cells (%)
-
shNT
sh1
sh2
E
SUM1315MO2 controls
Transiently expressed BRCA1 variants
ΔRING
WT
kDa
268
238
WT
M48
M128
M297
AB BRCA1 aa 1005-1313
hBRCA1
hBRCA1 ΔRING
AB BRCA1 aa 1-304
F
Endogenous BRCA1 expression (%)
160
140
120
100
80
60
40
20
0
NTF shNT
NTF sh1
WT shNT
WT sh1
M48 shNT
M48 sh1
M128 shNT
M128 sh1
M297 shNT
M297 sh1

Figure S7, related to figure 7

Functional importance of RING-less BRCA1 proteins in human tumor cells. (A) Colony formation of *BRCA1*^{185delAG} mutant SUM1315MO2 tumor cells after hBRCA1 knockdown with two different shRNAs (sh1, sh2) or a non-targeting control (shNT). (B) Relative metabolic activity of *BRCA1*^{185delAG} mutant SUM1315MO2 tumor cells after hBRCA1 knockdown. Medium: no cells, negative control. Metabolic activity was measured using resazurin and normalized to SUM1315MO2 cells transduced with shNT. SUM1315 shNT vs. sh1 or sh2 unpaired two-tailed t test $p<0.0001$. Error bars indicate SD. (C) Representative images of RAD51 IRIF in SUM1315MO2 cells after hBRCA1 knockdown. The pictures on the right are single-cell zoom-ins of the cells indicated with the red triangle. (D) EdU incorporation in gamma irradiated *BRCA1*^{185delAG} mutant SUM1315MO2 tumor cells with or without hBRCA1 knockdown. non-transduced cells (-) and shNT, sh1 or sh2 transduced cells were evaluated and results are representative of two independent experiments. Statistical analysis by Fischer's exact test revealed no significant differences in the percentages of cells in S/G2 phases as identified by EdU incorporation. (E) Western blot analysis of (left panel – part of Figure 5B) SUM1315MO2 cells expressing the endogenous RING-less BRCA1 protein or stably transfected with BRCA1 wild-type cDNA (WT) and sh1, targeting the endogenous BRCA1 3' UTR and (right panel) HEK 293T cells transiently transfected with wild-type BRCA1 and N-terminal truncation variants BRCA1-M48, -M128 and M297. (F) QRT-PCR analysis of endogenous *BRCA1* mRNA expression in BRCA1 complemented *BRCA1*^{185delAG} SUM1315MO2 cells. SUM1315MO2 cells were stably transfected with wild-type BRCA1 (WT) or N-terminal truncation variants BRCA1-M48, -M128 and -M297 and subsequently lentivirally transduced with a non-targeting shRNA (shNT) or *BRCA1*-3'UTR targeting shRNA sh1. NTF = non-transfected SUM1315MO2 cells. *BRCA1*-3'UTR containing mRNA was detected using a forward primer in exon 22 and a reverse primer in the 3'UTR of *BRCA1*. Levels were corrected for *RPL13* expression and normalized to the non-transfected control. Error bars indicate SD and data are representative for two independent experiments.

Figure S8A-C

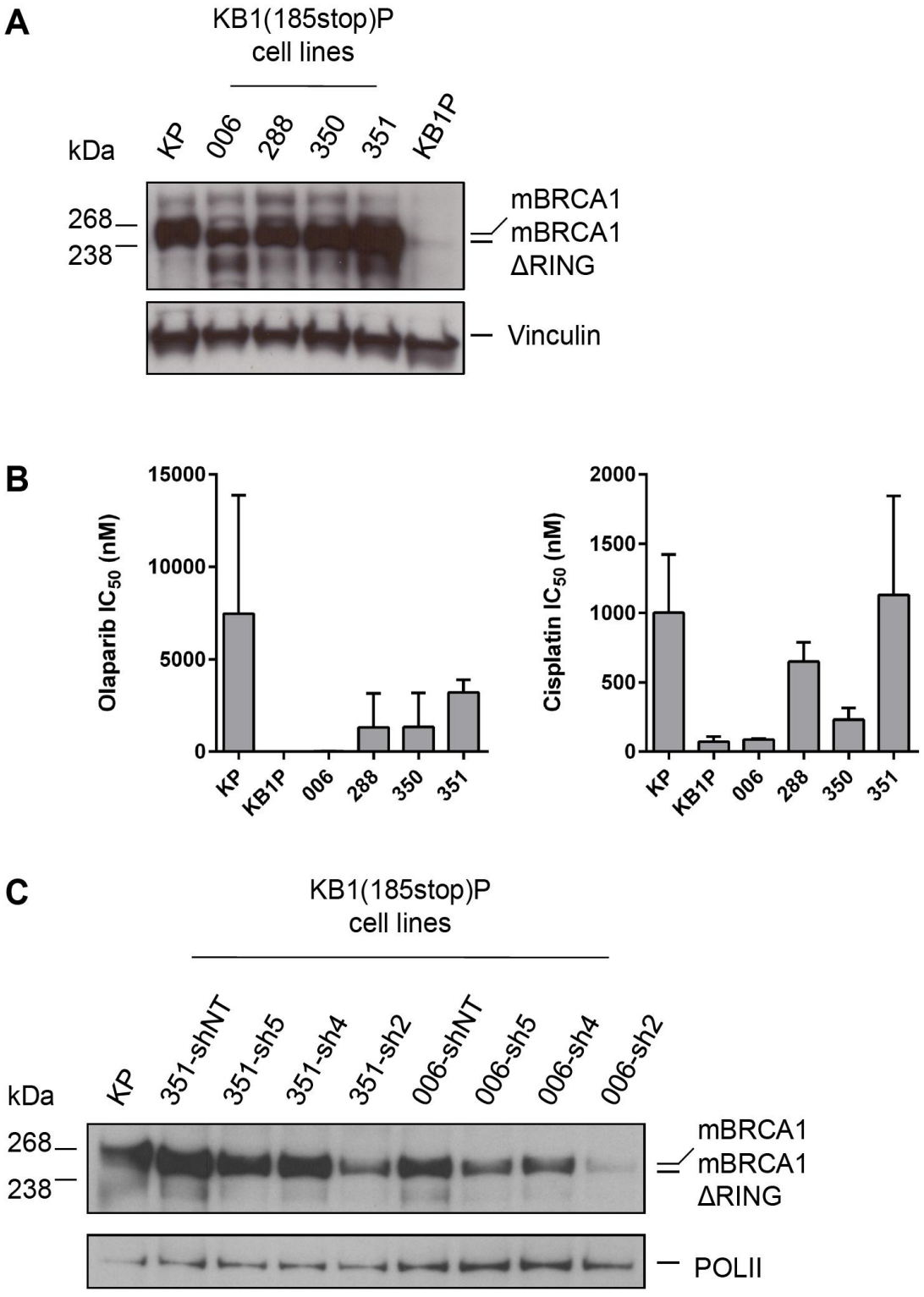
A
KB1(185stop)P
cell lines
kDa
KP
006
288
350
351
KB1P
268
238
mBRCA1
mBRCA1
ΔRING
Vinculin
B
Olaparib IC50 (nM)
15000
10000
5000
0
KP
KB1P
006
288
350
351
Cisplatin IC50 (nM)
2000
1500
1000
500
0
KP
KB1P
006
288
350
351
C
KB1(185stop)P
cell lines
kDa
KP
351-shNT
351-sh5
351-sh4
351-sh2
006-shNT
006-sh5
006-sh4
006-sh2
268
238
mBRCA1
mBRCA1
ΔRING
POLII

Figure S8D

D

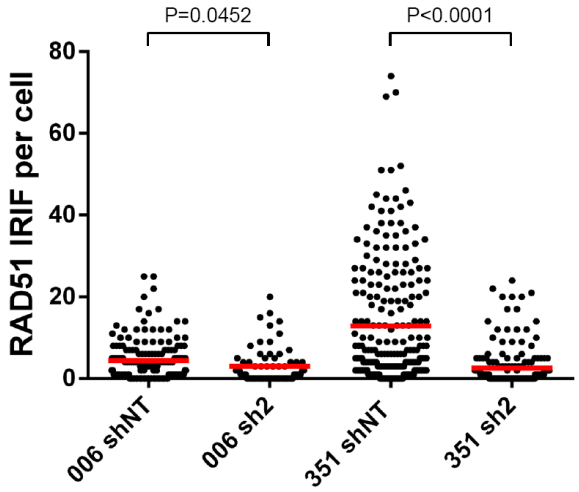

Figure S8, related to figure 7

Characterization of *KB1(185stop)P* mouse mammary tumor cell lines.

(A) Western blot analysis of mouse (m) BRCA1 protein expression in *KB1(185stop)P* mouse mammary tumor cell lines and BRCA1 positive *KP*3.33 (*KP*) and negative *KB1P* B11 (*KB1P*) controls. (B) Cisplatin and olaparib IC_{50} values of *KB1(185stop)P* cell lines 006, 288, 350 and 351, compared to *KP* and *KB1P* controls. Error bars indicate SD for two independent experiments. (C) Western blot analysis of *Brca1* knockdown efficiency in *KB1(185stop)P* 006 and 351 cell lines. Three different shBrca1 constructs (sh2, sh4, sh5) were compared to a non-targeting shRNA control (shNT). POLII expression was used as loading control. (D) Quantification of RAD51 IRIF in *KB1(185stop)P* mouse mammary tumor cell lines 006 and 351 lentivirally transduced with shNT or sh2. Statistically significant decreases in RAD51 IRIF formation upon knockdown of *Brca1* in over 70 *KB1(185stop)P* 006 ($p=0.0353$) and 351 cells ($p<0.0001$) were calculated using an unpaired two-tailed t test.

Figure S9A-D

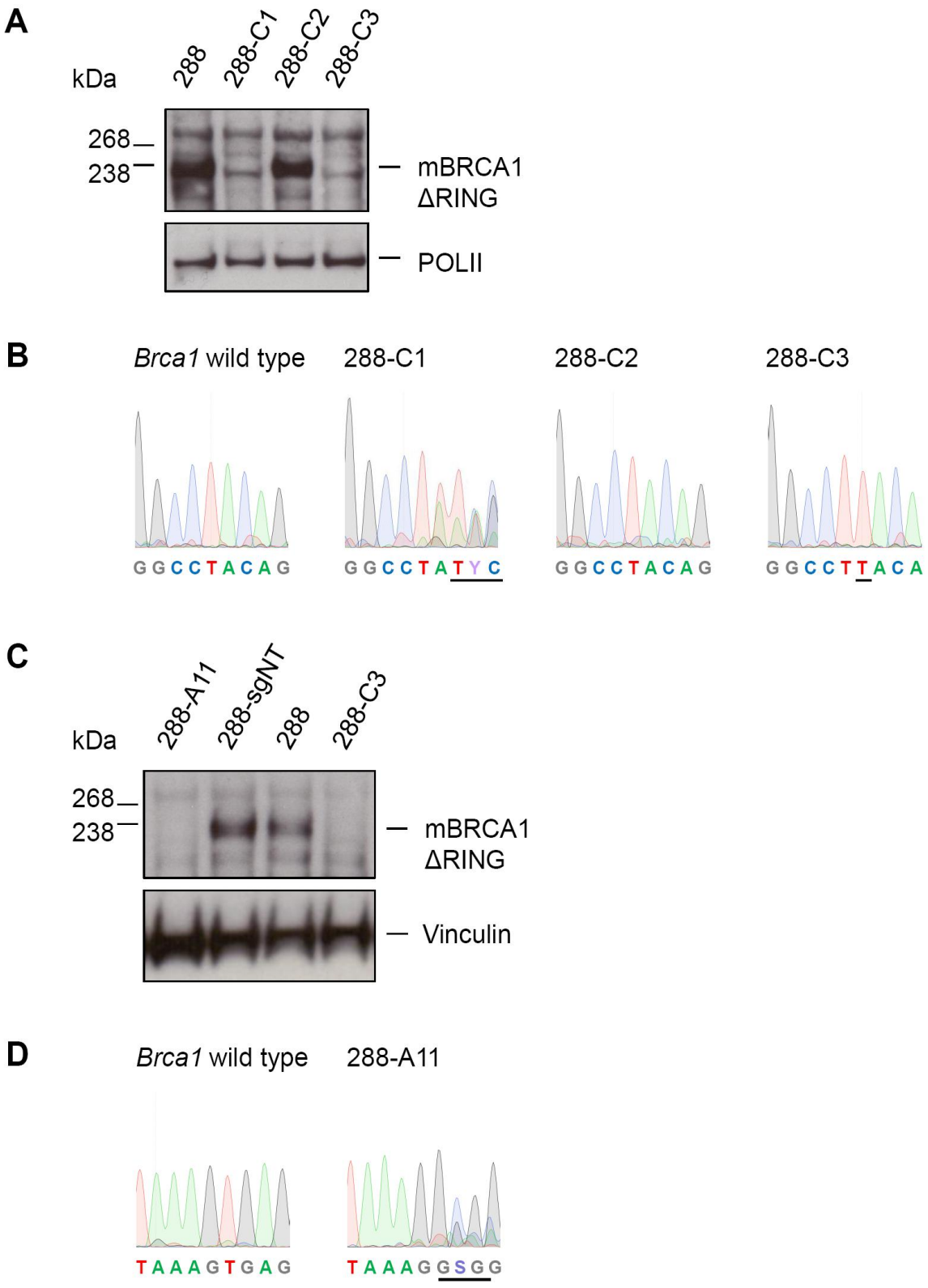
A
kDa
288
288-C1
288-C2
288-C3
268
238
mBRCA1
ΔRING
POLII
B
Brca1 wild type
288-C1
288-C2
288-C3
G G C C T A C A G
G G C C T A T Y C
G G C C T A C A G
G G C C T T A C A
C
kDa
288-A11
288-sgNT
288
288-C3
268
238
mBRCA1
ΔRING
Vinculin
D
Brca1 wild type
288-A11
T A A A G T G A G
T A A A G G S G G

Figure S9E-F

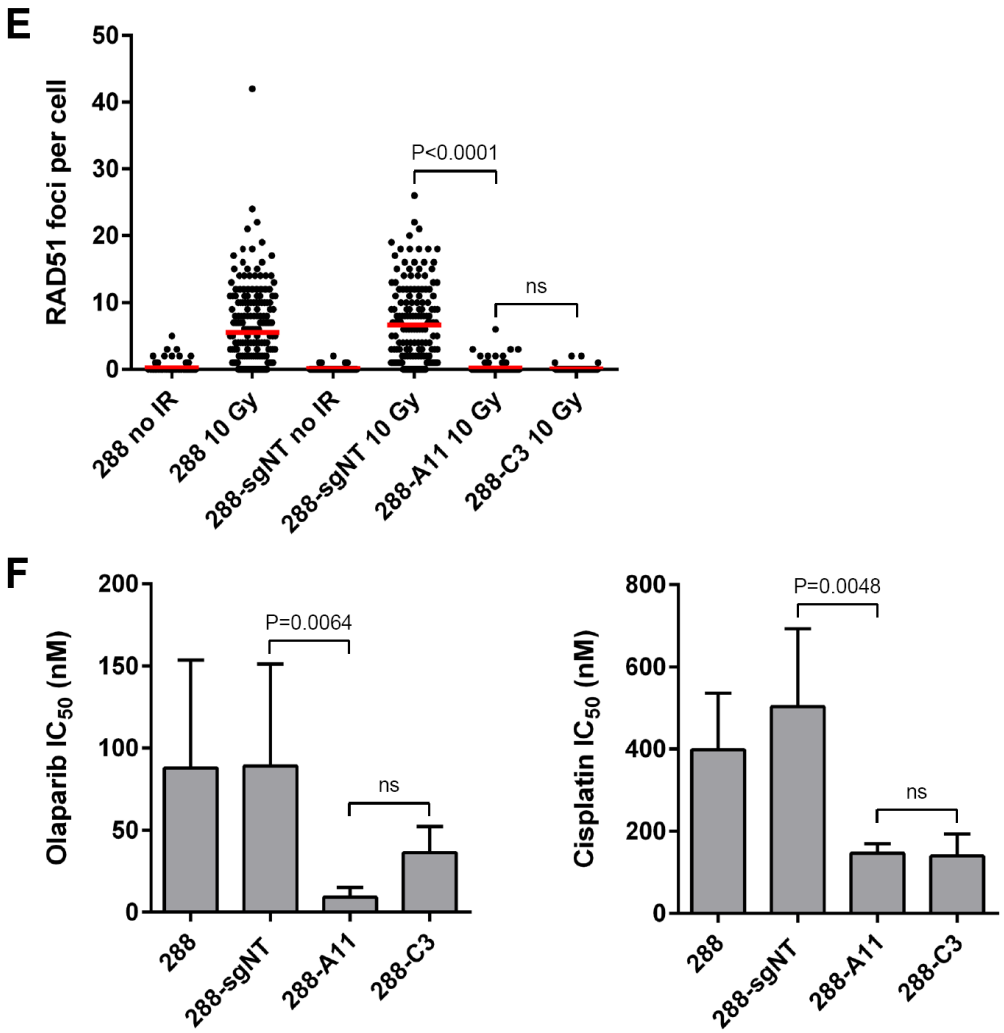

Figure S9, related to figure 7

Functional importance of RING-less BRCA1 for the response to homologous recombination deficiency targeting therapy.

(A) Western blot analysis of BRCA1 protein expression in subclones C1-3 of CRISPR/Cas9 sg1 targeted *KB1(185stop)P* 288 cells compared to non-targeted 288 cells. Expression of POLII was used as a loading control. (B) Sequence plots of the CRISPR/Cas9 sg1 targeted region of *KB1(185stop)P* 288 subclones C1-3 and a *Brca1* wild type control. Frameshift introducing alterations in the BRCT encoding region of 288-C1 and 288-C3 cells are underlined. (C) Western blot analysis of BRCA1 protein expression in subclone A11 of *KB1(185stop)P* 288 cells targeted with CRISPR/Cas9 sg2 compared to a control transfected with a non-targeting gRNA (sgNT), 288 and 288-C3 cells. Expression of Vinculin was used as a loading control. (D) Sequence plots of the CRISPR/Cas9 sg2 targeted region of *KB1(185stop)P* 288 subclone A11 and a *Brca1* wild type control. Reading frame altering mutations in KB1(185stop)P 288 cells and the BRCT encoding region of 288-A11 are underlined. (D) Analysis of RAD51 IRIF formation in *KB1(185stop)P* 288, 288-sgNT, 288-A11 and 288-C3 cells. Cells were irradiated with 10 Gy and RAD51 foci formation in S/G2 was compared to non-irradiated controls (no IR). Red bars indicate mean number of foci in over 80 evaluated cells, p values were determined using an unpaired two-tailed t test and data are representative for two independent experiments. (F) Olaparib and cisplatin IC_{50} values of *KB1(185stop)P* cell line 288 and subclones 288-sgNT, 288-A11 and 288-C3. Error bars indicate SD of three (288-C3) or four (288, 288-sgNT, 288-A11) independent experiments.

Figure S10A-C

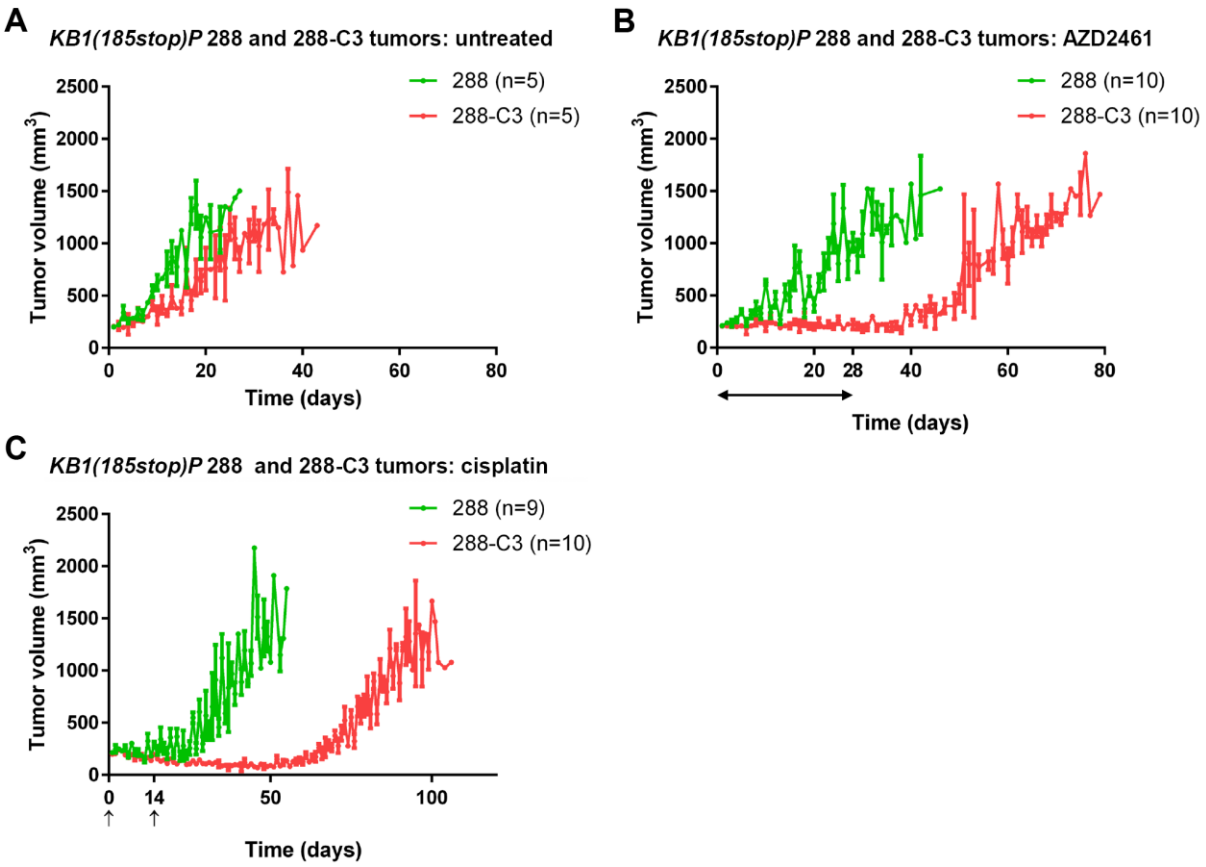

Figure S10, related to figure 7

Growth and treatment response of *KB1(185stop)P* mouse mammary tumors with or without expression of RING-less BRCA1.

(A-C) Growth comparison and treatment response of mammary tumors derived from the *KB1(185stop)P* 288 cell line and its *Brca1* deficient 288-C3 subclone. Average tumor volumes are shown from ± 200 mm^3 (day 0) onwards. Error bars indicate SEM. (A) Untreated controls. (B) Response to treatment with the PARP inhibitor AZD2461. Mice were treated with 100 mg/kg AZD2461 for 28 consecutive days as indicated by the arrow. (C) Response to cisplatin treatment. Mice were treated with 6 mg/kg cisplatin at day 0 and day 14 as indicated by arrows.

Figure S11A-C

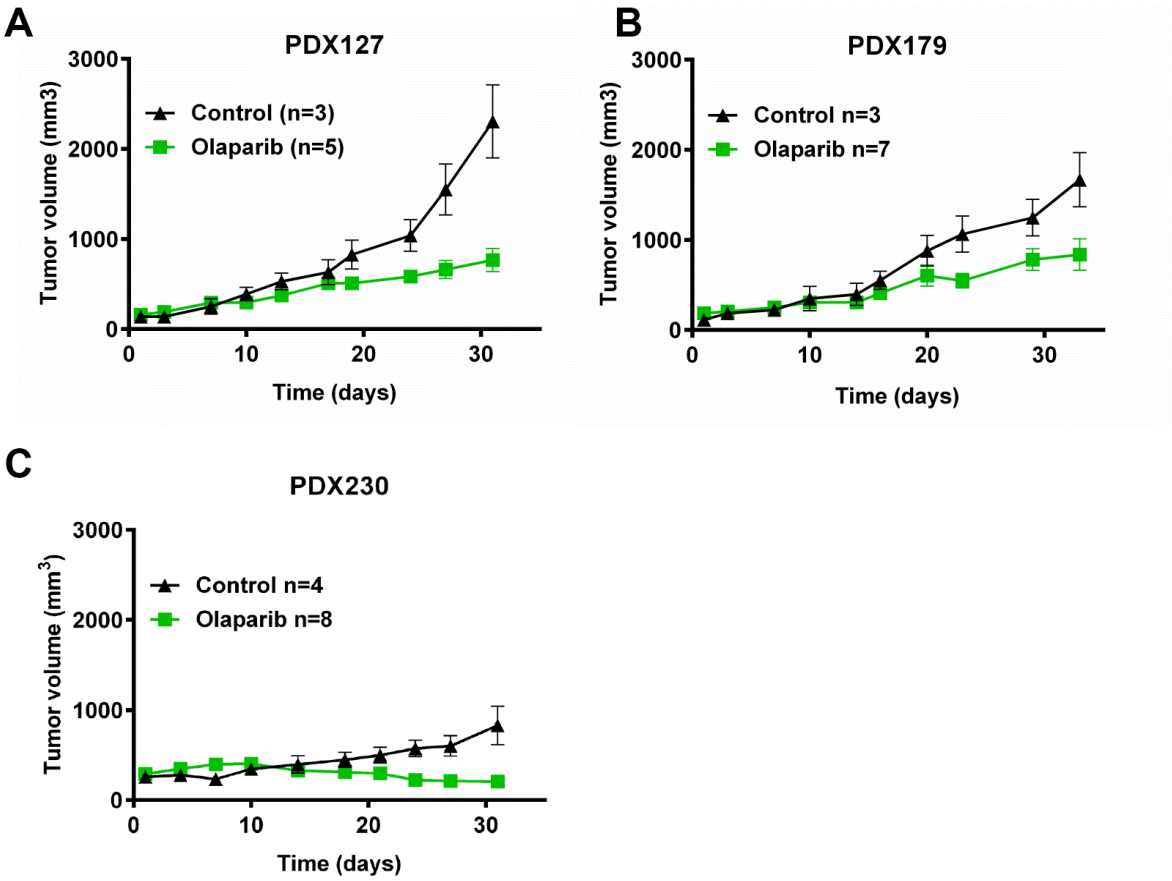

Figure S11, related to figure 8

Olaparib response of three different *BRCA1*^{185delAG} PDX models of breast cancer.

(A-C) Tumor growth of three different *BRCA1*^{185delAG} PDX models of breast cancer, PDX127 (A), PDX179 (B) and PDX230 (C), with and without olaparib treatment. Transplanted tumors were injected intraperitoneally with 50 mg/kg olaparib or vehicle (control) from day 1. Error bars indicate SEM.

Supplemental Methods

Generation of the Brca1^{185stop} and Brca1^{5382stop} mutant mice

The following primers were used to identify mutant mESCs by PCR:

Brca1^{185stop} PCR 1:

185stop fwd1	5′-CAA GTC CAG TGT GGG ATG-3′
185stop rev1	5′-CCT GGT GCA GTA GCT TAA AC-3′

Brca1^{185stop} PCR 2 (nested):

185stop fwd2	5′-CAC TAG GGT GGA AAC TGG T-3′
185stop wild type rev	5′-TCC GAT CTG GTA AGT CAA CA-3′
185stop mutant rev	5′-AAG GAT CTG GTA AGT CAA CAG-3′
185stop rev2	5′-TTC AAG TTG GAG GCT AAT C-3′
185stop wild type fwd	5′-ATG CAG AAA ATC TTA GAG TGT CC-3′
185stop mutant fwd	5′-GCA GAA AAT CTT AGA GTG AAG-3′

Brca1^{5382stop} PCR 1:

5382stop fwd1	5′-CCT TTT GTG TTT CCT GCA CC-3′
5382stop rev1	5′-CAG GGT TTT ATT CCA GCA GC-3′

Brca1^{5382stop} PCR 2 (nested):

5382stop fwd2	5′-CTT GGA CCT CAG AGA TGG G-3′
5382stop wild type rev	5′-ATC CAG AGA ATC CCG GG-3′
5382stop mutant rev	5′-GCG ATC CAG AGA ATC AGG A-3′
5382stop rev2	5′-CCT CAT GGG TTC TCA CAG C-3′
5382stop wild type fwd	5′-ATC CCG GGA AAG GTA AAG-3′

5382stop mutant fwd 5’-AGG ACC GGG AAA AGG TAA AG-3’

Cell culture

Mouse mammary tumor cell lines were established from freshly isolated mouse mammary tumors as previously described (1, 2) and grown under low oxygen (3%) conditions in DMEM-F12 culture medium (Gibco Invitrogen) supplemented with 10% (v/v) fetal bovine serum (FBS; Sigma Aldrich), 1% (v/v) penicillin-streptomycin (50U/ml penicillin, 50µg/ml streptomycin; Gibco Invitrogen), 5 µg/ml insulin (Sigma Aldrich), 5 ng/ml epidermal growth factor (EGF; Invitrogen) and 5 ng/ml cholera toxin (Gentaur). SUM1315MO2 (*BRCA1*^{185delAG}) cells (3) (provided by Mieke Schutte, Erasmus MC, Rotterdam, NL or Asterand Bioscience) and cisplatin-resistant clones were cultured in RPMI culture medium (Gibco Invitrogen) supplemented with 10% (v/v) FBS (Sigma Aldrich) and 1% (v/v) penicillin-streptomycin or in Ham’s F12 media (Gibco Invitrogen) with 5% (v/v) FBS (Hyclone), 5 µg/ml insulin, 10 ng/ml EGF (Sigma Aldrich), 10 mM Hepes (Sigma Aldrich), L-glutamine (Gibco Invitrogen) and 1% (v/v) penicillin-streptomycin. HCC1937 (*BRCA1*^{5382insC}) (4) (ATCC) and HCC1937+BRCA1 cells (provided by Paul Andreassen, Cincinnati Children's Research Foundation, Cincinnati, USA) were grown in RPMI culture medium supplemented with 10% (v/v) FBS (Sigma Aldrich) and 1% (v/v) penicillin-streptomycin or in RPMI with 15% (v/v) FBS (Hyclone), L-glutamine and 1% (v/v) penicillin-streptomycin. SUM149PT (*BRCA1*^{2288delT}) cells (3) (Asterand Bioscience) were cultured in Ham’s F12 media with 5% (v/v) FBS (Hyclone), 5 µg/ml insulin, 1 µg/ml hydrocortisone (Sigma Aldrich), 10mM Hepes, L-glutamine and 1% (v/v) penicillin-streptomycin. U2OS cells (ATCC) were cultured in DMEM (Gibco Invitrogen) with 10% (v/v) FBS (Hyclone), L-glutamine and 1% (v/v) penicillin-streptomycin.

To generate SUM1315MO2 clones with increased cisplatin-resistance, cells were treated with 12.5 or 25 mM cisplatin (Sigma Aldrich, P4394) for 1 h. Cells were allowed to recover and expanded prior to selection in 0.5 to 1.0 mM cisplatin for 8 weeks. Colonies remaining at the end of selection were picked and expanded for further analysis.

Generation of mouse mammary tumors and orthotopic transplantations

All experiments involving genetically engineered mouse models comply with local and international regulations and ethical guidelines, and have been authorized by our local animal experimental committee at the Netherlands Cancer Institute (DEC-NKI). The generation of *KP and KB1P* mice has been described previously (5, 6).

Brca1$^{185stop/+}$ and *Brca1*$^{5382stop/+}$ mice were bred with *KB1P* animals to generate *K14cre;Brca1*$^{185stop/F}$*;p53*$^{F/F}$ (*KB1(185stop)P*), *K14cre;Brca1*$^{5382stop/F}$*;p53*$^{F/F}$ (*KB1(5382stop)P*) and littermate control mice. These animals were checked weekly from the age of 4 months onward for onset of tumor growth and overall appearance. After tumor onset, mammary tumor size was determined biweekly by caliper measurements. Tumors were harvested at a maximal size of 1000 mm^3 (formula tumor volume: 0.5 x length x width^2). FVB/n:129/Ola F1 hybrid or NMRI nude females were used for orthotopic transplantations of mammary tumors. Small tumor fragments (1-2mm in diameter) or mouse mammary tumor cell lines (500,000 in 50 µl PBS and growth factor reduced Matrigel (BD Biosciences) 1:1) were transplanted orthotopically in the fourth mammary fat pad of adult female mice as described (7, 2).

Treatment of mouse mammary tumor-bearing animals

Maximum tolerable dose (MTD) levels of cisplatin and olaparib and the effective dose of AZD2461 were determined in earlier studies (7, 2, 8). 6 mg/kg of cisplatin (Mayne Pharma; 1 mg/ml in saline-mannitol) was administered by intravenous injection in the tail vein. For olaparib (kindly provided by AstraZeneca) 50 mg/ml stocks in DMSO were diluted 10-fold in 10% (w/v) 2-hydroxyl-propyl-β-cyclodextrine/PBS and for AZD2461 a 10 mg/ml suspension in 0.5% (w/v) 2-hydroxyl-propyl-β-cyclodextrine/PBS was used. 50 mg/kg of olaparib or 100 mg/kg AZD2461 was administered daily for 28 consecutive days by intraperitoneal injection or *per os* respectively. Treatment at MTD levels was initiated when the tumor volume, calculated as 0.5 x length x width^2, exceeded 200 mm^3. Of note, all cohorts transplanted with tumor pieces were treated simultaneously and the results of the *KP* and *KB1P* control cohorts have been reported previously (9). To

determine whether tumors would acquire resistance to cisplatin, animals received multiple doses of cisplatin. An animal was retreated two weeks after the initial treatment if the tumor volume was larger than 50%. If the tumor volume was smaller than 50% two weeks after the initial treatment, an animal was not retreated until the tumor volume reached 100%. Animals were sacrificed when the tumor volume exceeded 1500 mm^3 or because of severe weight loss due to toxicity of the drug.

DNA isolation, southern blot analysis and genotyping

For routine genotyping, tail DNA samples or yolk sacs were lysed in DirectPCR lysis reagent (Viagen) supplemented with 100 μg/ml proteinase K (Sigma Aldrich). The *Brca1*^{F} allele was detected by PCR amplification of the loxP site in intron 3 with primers *P1* and *P2*, yielding products of 545 bp and 390 bp for the floxed and wild type alleles, respectively. Detection of the *Brca1*^{del} allele with primers *P1* and *P3* yielded a 594-bp fragment. The primer sequences were as follows: *P1*, 5'-TAT CAC CAC TGA ATC TCT ACC G-3'; *P2*, 5'-GAC CTC AAA CTC TGA GAT CCA C-3' and *P3*, 5'-TCC ATA GCA TCT CCT TCT AAA C-3'. For all PCR reactions, thermocycling conditions consisted of 30 cycles of 30 sec at 94°C, 30 sec at 58°C, and 50 sec at 72°C. Reactions contained approximately 200 ng of template DNA, 0.5 mM primers, 100 mM dNTPs, 2.5 units of *Taq* DNA polymerase, 2.5 mM $MgCl_2$, and 10 x PCR buffer in a total volume of 20 µl. The *Brca1*^{185stop} and *Brca1*^{5382stop} alleles were detected by probe-based melting curve analysis. For high-resolution melting curve analysis, we used the LightCycler 480 instrument of Roche Applied Science. We used the following probes and primers for melting curve genotyping:

Brca1^{185stop}:

Anchor HybProbe	5'-AAG ATT TTC TGC ATA GCA TGA AGG ACA TTT TGT AC--PH
Sensor HybProbe	5'-CTG TTG ACT TAC CAG ATC GGA CAC TC--FL
Primer forward	5'-CTC ATT TGC ATG AAC AGT AAC CAC-3'
Primer reverse	5'-TTA TCT GCC GTC CAA ATT CAA G-3'

Brca1^{5382stop}:

Anchor HybProbe	5’-ATC GCC TTG GAC CTT GGT GAT TTC TTC C--PH
Sensor HybProbe	5’-CTT TTC CCG GTC CTG ATT CTC TG--FL
Primer forward	5’-TTA GGC TGG GGT TCT GTC-3’
Primer reverse	5’-TTG AAG TCA AAG GAG ATG TTG T-3’

After 10 min pre-incubation at 95 °C, thermocycling conditions for high-resolution melting curve analysis consisted of 45 cycles of 10 sec at 95 °C, 10 sec at 60 °C, and 10 sec at 72 °C. Afterwards, a melting curve was produced by 1 min incubation at 95 °C and 2 min incubation at 40 °C. Reactions contained approximately 200 ng of template DNA, 5 pmol forward primer, 20 pmol reverse primer, 3 pmol sensor probe, 3 pmol anchor probe, and 2 x LightCycler 480 Probes Master (Roche Applied Science) in a total volume of 20 µl.

Sanger sequencing

The following primers were used for sequencing on DNA:

Brca1^{185stop}*:*

185stop fwd1	5’-CAA GTC CAG TGT GGG ATG-3’
185stop fwd2	5’-CAC TAG GGT GGA AAC TGG T-3’
185stop rev1	5’-CCT GGT GCA GTA GCT TAA AC-3’
185stop rev2	5’-TTC AAG TTG GAG GCT AAT C-3’

Brca1^{5382stop}:

5382stop fwd1	5’-CCT TTT GTG TTT CCT GCA CC-3’
5382stop fwd2	5’-CTT GGA CCT CAG AGA TGG G-3’
5382stop rev1	5’-GGT TTT ATT CCA GCA GC-3’
5382stop rev2	5’-CCT CAT GGG TTC TCA CAG C-3’

The following primers were used for sequencing on cDNA:

Brca1^{185stop}*:*

mBrca1 ex1 fwd 5′-CTT GGG GCT TCT CCG TCC TC-3′

mBrca1 ex2 fwd 5′-ACT GGA ACT GGA AGA AAT GG-3′

mBrca1 ex4/5 rev 5′-TGT AGG CTC CTT TTG GTT AT-3′

mBrca1 ex5 rev 5′-CTT GTG CTT CCC TGT AGG-3′

Brca1^{5382stop}:

mBrca1 ex12 fwd 5′-CCA AAC ATG TCA GGA GCA-3′

mBrca1 ex14 fwd 5′-TTC AAC AGG GCA GTC TTG-3′

mBrca1 ex18 fwd 5′-GGT CCG GTC TAT CCA AGA-3′

mBrca1 ex20 rev 5′-GGC TCA CAA CAA TAG ACC TG-3′

mBrca1 ex24 rev 5′-TTC TGT ACC AGG TAG GCA TC-3′

RNA isolation and RT-PCR analysis

Total RNA from cell lines and mouse tissues was isolated using Trizol (Invitrogen). The integrity of RNA was verified by denaturing gel electrophoresis. Before cDNA synthesis, RNA samples were treated with RQ1 RNase-free DNase (Promega) to degrade both double- and single stranded DNA and with RNasin (Promega) to inhibit activity of RNases. Subsequently, cDNA was synthesized using random hexamer primers and cloned AMV reverse transcriptase (Invitrogen). RT-PCRs were performed using the following primers:

Mouse Brca1 ex10 forward	5′-GAG ATG AAG GCA AGC TGC-3′
Mouse Brca1 ex11 reverse	5′-CAG TTG CAT GAT TCT CAG TAG G-3′
Mouse HPRT forward	5′-CTG GTG AAA AGG ACC TCT CG-3′
Mouse HPRT reverse	5′-TGA AGT ACT CAT TAT AGT CAA GGG CA-3′
Human BRCA1 3′UTR forward	5′-AGC TGT GTG GTG CTT CTG TG-3′
Human BRCA1 3′UTR reverse	5′-AAG CTC ATT CTT GGG GTC CT-3′

Human RPL13 forward	5’-GAG ACA GTT CTG CTG AAG AAC TGA A-3’
Human RPL13 reverse	5’-TCC GGA CGG GCA TGA C-3’

LightCycler 480 SYBR Green I Master (Roche Applied Science) or SensiMix SYBR Low_ROX (Bioline) were used for amplification and detection of cDNA target. RT-PCR was carried out on the LightCycler 480 instrument of Roche Applied Science or on the Applied Biosystems 7500 Fast Real-Time PCR System.

Array comparative genome hybridization and data analysis

Genomic DNA of tumor and spleen samples was extracted by proteinase K lysis and organic extraction with phenol-chloroform. Tumor and spleen samples were labeled with the Nimblegen dual-color DNA labeling kit and hybridized to the Nimblegen 12-plex 135K full genome mouse custom NKI array. Background correction and normalization was performed in the NimbleScan program. Probe annotation and corrected log2 ratios were imported into the R programming language from the NimbleScan output. Probes mapping to Y and mitochondrial chromosomes were discarded. To find genomic loci of significant difference between the groups of tumors we applied the comparative module of the R package KCsmart (as available in BioConductor; (10, 11)). All comparisons were performed using standard parameters (sigma = 1 Mb, 1000 permutations, $p < 0.05$). In short: a smoothed profile for each individual tumor was computed. The SAM algorithm as implemented in the multitest R-package was used to calculate significantly different copy number changes for discrete sample points along the mouse genome.

Antibodies

The following primary antibodies were used for immunohistochemistry: rat anti-cytokeratin 8 (University of Iowa Troma-1; 1:600), rabbit anti-vimentin (Abcam ab45939; 1:1500), rabbit anti-progesterone receptor (Neomarkers RM-9102-SO; 1:300), and rabbit anti-estrogen receptor alpha (Santa Cruz Biotechnology SC-542; 1:1750) and rabbit anti-53BP1 (Bethyl laboratories A300-272A; 1:1000). The following secondary

antibodies were used for immunohistochemistry: biotin-conjugated anti-rat (Santa Cruz Biotechnology SC-2041; 1:100), biotin-conjugated anti-rabbit (Dako E0432; 1:1000) and HRP-conjugated anti-rabbit Envision (Dako K4009). The following primary antibodies were used for western blot analysis: mouse anti-BRCA1 (Abcam ab16780, MS110; epitope human BRCA1 aa 1-304; 1:250), mouse anti-BRCA1 (Santa Cruz Biotechnology sc-6954, D-9; epitope human BRCA1 aa 1842-1862; 1:200), rabbit anti-BRCA1 (Cell Signaling Technology 9010; epitope human BRCA1 305-325; 1:1000), mouse anti-BRCA1 (EMD Millipore OP107, SD118; epitope human BRCA1 aa 1005-1313; 1:250), rabbit anti-BRCA1 (12) (epitope mouse BRCA1 aa 452-469; 1:500; provided by Ronny Drapkin, University of Pennsylvania, Philadelphia, USA), mouse anti-BRCA1 (13) (epitope mouse BRCA1 aa 1365-1812; 1:10), rabbit anti-53BP1 (Abcam ab21083; 1:1000), rabbit anti-Actin (Santa Cruz Biotechnology SC-1616R; 1:10000), mouse anti-Vinculin (Sigma Aldrich hVIN-1; 1:10000) and goat anti-POLII (Santa Cruz Biotechnology C-18; 1:200). The following secondary antibodies were used for western blot analysis: HRP-conjugated rabbit anti-goat (Dako; 1:1000), HRP-conjugated rabbit anti-mouse (Dako; 1:2500) and HRP-conjugated goat anti-rabbit (Dako; 1:2000). Rabbit anti-RAD51 (1:10000; provided by Roland Kanaar, Erasmus MC, Rotterdam, NL) or rabbit anti-RAD51 H-92 (Santa Cruz Biotechnology; 1:500) and mouse anti-Brca1 (13) (1:10) were used as a primary antibodies for immunofluorescence studies. Goat anti-rabbit Alexa fluor 568 (Invitrogen; 1:400) and Goat-anti-mouse Alexa fluor 488 (Invitrogen; 1:400) were used as secondary antibodies for immunofluorescence studies. For the alpha track assay the following primary antibodies were used: rabbit anti-53BP1 (Novus NB100-304; 1:1000), mouse anti-RPA2 (Abcam Ab2175; 1:500). Secondary antibodies were goat anti-rabbit Alexa fluor 594 (Invitrogen; 1:1000) and goat anti-mouse Alexa fluor 488 (Invitrogen; 1:1000). For RAD51 immunofluorescence on PDX samples we used rabbit anti-RAD51 (Santa Cruz Biotechnology H-92; 1:250), mouse anti-Geminin (NovoCastra NCL-L; 1:100) and goat anti-rabbit Alexa Fluor 568 or goat anti-mouse Alexa Fluor 488 secondary antibodies (Invitrogen; 1:500).

Histology and immunohistochemistry

Tissues were isolated and fixed in formaldehyde for 48 h. Tissues were rehydrated, cut into 4 µm sections and stained with hematoxylin and eosin. For immunohistochemical staining for progesterone receptor and cytokeratin 8, antigen retrieval was performed with citra solution (Biogenex HK086-5K). For immunohistochemical staining for estrogen receptor alpha, antigen retrieval was performed with 0.05% (w/v) citraconic anhydride (Fluka 27429). For immunohistochemical staining for vimentin, antigen retrieval was performed with Tris/EDTA pH 9.0. Subsequently, endogenous peroxidases were blocked with 3% (v/v) H_2O_2. Before slides were incubated with vimentin primary antibody, slides were pre-incubated with 1% (w/v) milk/PBS. Before slides were incubated with primary antibody for progesterone receptor, slides were pre-incubated with PBS with 4% (w/v) BSA and 5% (v/v) normal goat serum (Sanquin). Next, slides were incubated with HRP-conjugated Envision (Dako) or stained with biotin-conjugated secondary antibodies and incubated with HRP-conjugated streptavidin-biotin complex (Dako). Following detection with 3,3-diaminobenzidine-tetrahydrochloride (DAB; Sigma Aldrich, A-6926), slides were counterstained with heamatoxylin and dehydrated. Tumors were only scored positive for ER or PR, when more than 10% of tumor cells stained positive.

Preparation of tumor cell suspensions for ex vivo analysis of RAD51 IRIF

Cryo-preserved tumors were cut into small pieces with sterile scalpels (Swann Morton) in PBS (Invitrogen) supplemented with 0.5 mM EDTA (Lonza). Subsequently, tumor pieces were digested with 0.1% (w/v) trypsin (Invitrogen) and 3 mg/ml collagenase A (Roche) for 30 min at 37 °C. Tumor cell suspensions were passed through a 40 µM cell strainer (BD Biosciences). After cell counting, appropriate amount of tumor cells were plated on glass coverslips (Omnilabo) and grown for 36-48 h at 37 °C in low oxygen (3%) condition.

BRCA1/RAD51/53BP1 immunofluorescence

Cells were irradiated with 10 Gy to induce repair foci at DNA DSBs. After irradiation, cells were incubated for 6 h at 37 °C, washed with PBS and fixed using 2-4% (w/v) paraformaldehyde (PFA; Merck) in PBS for 15-30 min at room temperature. Fixed cells were washed three times with PBS and stored at 4 °C. For permeabilization cells were incubated in 0.2-0.5% (v/v) Triton X-100 (Sigma Aldrich) in PBS and washed three times in staining buffer (PBS containing 0.5% (w/v) BSA (Sigma Aldrich), 0.15% (w/v) glycin (Fluka) and 0.1% (v/v) Triton X-100) for 5 min at a rocking plate. To block non-specific interactions, cells were incubated for 30 min in staining buffer at room temperature. Subsequently, cells were incubated with primary antibodies for 2 h at room temperature. After three washes in staining buffer, cells were incubated with secondary antibodies for 1 h at room temperature. After three additional washes in staining buffer, coverslips were mounted in Vectashield H1500 with DAPI (Vector Laboratories) or stained with DAPI (Invitrogen; 0.5 µg/ml in staining buffer) for 5 min at room temperature, washed once in staining buffer and mounted in Vectashield H1000 (Vector Laboratories).

Alternatively, when performing Click-iT chemistry (Invitrogen), 20 µM EdU was added to the medium of cultured cells 1 h before for fixation. Permeabilized cells were rinsed twice in PBS with 3% (w/v) BSA before EdU detection according to protocol of the Click-iT EdU Alexa Fluor 594 imaging kit. Subsequently, cells were rinsed once in PBS with 3% (w/v) BSA and rinsed three times and washed twice for 10 min in PBS with 0.1% (v/v) Triton X-100. After rinsing the cells once in PBS+ (PBS containing 0.5% (w/v) BSA and 0.15% (w/v) glycin), samples were incubated for 1.5-2 h with primary antibodies in PBS+ at room temperature. Cells were then rinsed three times and washed twice for 10 min in PBS with 0.1% (v/v) Triton X-100, rinsed once in PBS+ and incubated for 1 h with the secondary antibody in PBS+. Finally, cells were rinsed three times and washed twice for 10 min in PBS with 0.1% (v/v) Triton X-100, rinsed once in PBS and mounted in Vectashield 1500 with DAPI.

Images were taken with a Leica TCS SP2 (Leica Microsystems) confocal system equipped with 405 diode, Argon, DPSS 561 and HeNe 633 lasers. Images were taken using a 63X

NA 1.32 objective. Standard LCS or LAS software was used for processing. In addition, pictures were taken using an AxioObserver Z1 inverted microscope (Zeiss) equipped with a cooled ORCA AG black and white CCD camera (Hamamatsu) and AxioVision 4.7.2 software (Zeiss). To quantify RAD51 foci in single tumor cells, 150-200 cells per condition were counted blindly using a 63x magnification lens. Cells were scored RAD51-positive if they had more than ten RAD51-positive dots per nucleus.

For automated analysis of RAD51 or 53BP1 foci, images were analyzed using an ImageJ macro that identified and counted nuclear foci. Briefly, nuclei were segmented by thresholding the (median-filtered) DAPI signal, followed by a watershed operation to separate touching nuclei. For every z-stack the maximum-intensity projection of the foci signal was background-subtracted using a Difference of Gaussians method. Next, for each nucleus, foci candidates were identified as locations where the resulting pixel values exceeded the background by a factor (typically 10-fold) times the median standard deviation of all nuclei in the image. In combination with additional filters discriminating for foci size and absolute brightness this procedure yielded a robust and reliable foci count for all nuclei. Results were validated by visual inspection. Cells in S/G2 phases of the cell cycle were labeled using EdU incorporation and Click-iT chemistry (Invitrogen). Graphpad Prism 6 was used to generate graphs and for the statistical analysis of the data.

RAD51 was quantified on FFPE PDX tumor samples by scoring the percentage of geminin positive cells with 5 or more RAD51 foci (14). Scoring was performed blindly onto live images. One-hundred geminin-positive cells from at least 3 different and representative areas of each sample were analyzed. Error bars indicate biological replicates.

Alpha track assay

Cells were seeded in mylar dishes as previously described (15), allowing α-particle irradiation through the bottom of the dish. 30 min, 1 h or 2 h post irradiation (3x 30 sec with a ^{241}Americium source), cells were washed once in ice-cold PBS. Next, cells were extracted with cold CSK buffer (10 mM Hepes KOH pH 7.9, 100 mM NaCl, 300 mM

Sucrose, 3 mM $MgCl_2$, 1 mM EGTA, 0.5% (v/v) Triton X-100) for 5 min and cold CSS buffer (10 mM Tris pH 7.4, 10 mM NaCl, 3 mM $MgCl_2$, 1% (v/v) Tween20, 0.5% (w/v) Sodium Deoxycholate) for 5 min before fixation in 4% (w/v) PFA in PBS for 15 min at room temperature. Fixed cells were washed five times in PBS+0.1% (v/v) Triton X-100 and washed once in blocking solution (0.5% (w/v) BSA + 0.15% (w/v) glycine in PBS). Primary antibodies were diluted in blocking solution and cells were incubated overnight at 4 °C while covered with parafilm. After incubation, cells were washed five times with PBS + 0.1% (v/v) Triton X-100 and washed once in blocking solution. Secondary antibodies were diluted 1:1000 in blocking solution and cells were incubated at room temperature for at least 1 h. Afterwards, cells were washed five times in PBS+0.1% (v/v) Triton X-100 and once in PBS. Finally, mylar films were glued on glass slides and cells were mounted using Vectashield with DAPI. For quantification, at least 100 53BP1 positive tracks were scored for the presence of RPA.

Ribosome profiling of tumor cell lines

To map translation start sites, cells were treated with 2 µg/ml of harringtonine (Santa Cruz) for 5 min and with 100 µg/ml of cycloheximide for 5 additional min. Cells were lysed in buffer containing 20 mM Tris-HCl, pH 7.8; 100 mM KCl; 10 mM $MgCl_2$; 1% (v/v) Triton X-100; 2 mM DTT; 100 µg/ml cycloheximide, and protease inhibitors. Lysates were digested with 2 U/µl of RNAse I (Ambion) for 40 min at room temperature. Monosomes were separated on a linear sucrose gradient using the SW-41Ti rotor at 36,000 rpm for 2 h. For libraries preparation, RNA was gel-purified on a denaturing 10% (w/v) polyacrylamide urea (7 M) gel. A section corresponding to 30 to 33 nucleotides was excised, eluted and ethanol precipitated. The resulting fragments were 3'-dephosphorylated using T4 PNK (NEB) for 6 h at 37 °C. 3' adaptor was added with T4 RNA ligase 1 (NEB) for 2.5 h at 37 °C. Ligation products were 5'-phosphorylated with T4 polynucleotide kinase for 30 min at 37 °C. 5' adaptor was added with T4 RNA ligase 1 for 18 h at 22 °C. The resulting fragments were purified and reverse transcribed using the

SuperScript III cDNA Synthesis Kit (Invitrogen). The cDNA was PCR amplified for 18 cycles and the libraries were sequenced in an Illumina HiSeq 2000 system.

Mass spectrometry analysis of mouse RING-less BRCA1 protein

Mouse BRCA1 was immunoprecipitated with the mBRCA1-16588 monoclonal antibody raised against the C-terminal part of mouse BRCA1 (13) and isolated from a NuPage 3-8% (w/v) polyacrylamide Tris Acetate gradient gel (Invitrogen) after staining with a colloidal coomassie G250 solution (16).

Excised 5 mm slices were subjected to destaining, in-gel reduction with dithiothreitol, alkylation with chloroacetamide and digestion with trypsin (Promega, sequencing grade), essentially as described (17). Nanoflow LC-MS/MS was performed on an 1100 series capillary LC system (Agilent Technologies) coupled to an LTQ-Orbitrap XL mass spectrometer (Thermo) operating in positive mode and equipped with a nanospray source. Peptide mixtures were trapped on a ReproSil C18 reversed-phase column (Dr Maisch GmbH; column dimensions $2\,\text{cm} \times 100\,\mu\text{m}$, packed in-house) at a flow rate of $8\,\mu\text{l}\,\text{min}^{-1}$. Peptide separation was performed on a ReproSil C18 reversed-phase column (Dr Maisch GmbH; column dimensions $20\,\text{cm} \times 75\,\mu\text{m}$, packed in-house) using a linear gradient from 0% to 80% B (A = 0.1% (v/v) formic acid; B = 80% (v/v) acetonitrile, 0.1% (v/v) formic acid) in 90 min and at a constant flow rate of $200\,\text{nl}\,\text{min}^{-1}$. The column eluent was directly sprayed into the ESI source of the mass spectrometer. Mass spectra were acquired in continuum mode; fragmentation of the peptides was performed in data-dependent mode by CID. Peak lists were created from raw data files using the Mascot Distiller software (version 2.3; MatrixScience). The Mascot algorithm (version 2.2; MatrixScience) was used for searching against a Uniprot database (releases 2012_11.fasta to 2013_04.fasta), taxonomy: Mus musculus (mouse) or a customized database containing BRCA1 and variants. The peptide tolerance was set to 10 p.p.m. and the fragment ion tolerance was set to 0.8 Da. A maximum number of two missed cleavages by trypsin were allowed and carbamidomethylated cysteine and oxidized methionine were set as fixed and variable modifications, respectively.

Transfections of cDNA constructs encoding human BRCA1 variants

Site-directed mutagenesis of *BRCA1* cDNA constructs to generate pcDNA3-based expression constructs for BRCA1 N-terminal truncation variants was performed as described (18). For western blot analysis of transiently expressed BRCA1 variants, HEK 293T cells were transfected overnight using calcium phosphate and harvested the next day. Stable transfections of SUM1315MO2 cells were performed using Lipofectamine 2000 (Invitrogen) and stably transfected cells were selected using 200 µg/ml G418 (Invitrogen).

hBRCA1 and mBrca1 knockdown experiments

Cells were transduced with pLKO-puro shRNA viruses obtained from TRC library clones (Thermo Scientific Open Biosystems). We used shRNAs targeting human *BRCA1* (TRCN0000039833 (#1, 3' UTR targeting), 5'-CCC TAA GTT TAC TTC TCT AAA-3'; TRCN0000010305 (#2, exon 11 targeting), 5'-AGA ATC CTAG AGA TAC TGA A-3'), mouse *Brca1* (TRCN0000042559 (#2, exon 11 targeting), 5'-GCT CAG TGT ATG ACT CAG TTT-3'; TRCN0000042561 (#4, exon 4 targeting), 5'-CCT TTG TGT AAG AAT GAG ATA-3'; TRCN0000042562 (#5, exon 11 targeting), 5'-CCA CAG GTA AAT CAG GAA TTT)-3'), and a nontargeting shRNA (SHC202, 5'-CAA CAA GAT GAA GAG CAC CAA-3'). After selection with 1.8 µg/ml puromycin, 1000 SUM1315MO2 cells per 6-well were seeded for clonal growth. After two weeks, cells were incubated for 4 h with CellTiter-Blue (Promega). Fluorescence (590 nm) and absorbance (570 and 600 nm) were measured by using the Infinite M200 microplatereader (Tecan). At the same time samples were taken for RNA and protein analysis. The cells were fixed in 4% (w/v) paraformaldehyde for 10 min and stained with 0.1% (w/v) crystal violet for 30 min.

CRISPR/Cas9-mediated inactivation of the Brca1^{185stop} allele

The Cas9 and gRNA expressing pX330 plasmid (19) was provided with a puromycin selection marker under control of the human *PGK* promoter. For inactivation of *Brca1*,

single guide RNAs against target sequence 5'-AGC TCT TCA AGG GCC TAC-3' in exon 21 and the preceding intron (sg1) and against target sequence 5'-CCT CAC TTT AAC TGA CGC AA-3' in exon 17 (sg2) were used. The target sequence for the non-targeting control sgNT was 5'-TGA TTG GGG GTC GTT CGC CA-3'. *KB1(185stop)P* mouse mammary tumor cells were transiently transfected using Lipofectamine 2000 (Invitrogen) and after overnight incubation, transfected cells were selected using 1.8 µg/ml puromycin for 2 days. Subsequently, cells were passaged, and after 4 days cells were seeded at clonal densitity. Before clones were picked, pools of transfected cells were analyzed by TIDE (20) for inactivation of the *Brca1*^{185stop} allele by sequence analysis of allele specific PCR products, generated with *Brca1* exon 12 forward (5'-TGA AGA CTG CTC GCA GAG TG-3') and exon 23/24 reverse (5'- CCA ATA TCT GGG CAG TTG CT 3') primers. Clones were analyzed for *Brca1*^{185stop} inactivation by sequencing using a primer in exon 16 (5'-TCA GAA GAA AGA GCG GAT AGA GA-3') and western blot analysis.

Clinical history of donor patients for PDX tumors

Patient 127 received neoadjuvant anthracycline/taxane-based chemotherapy for treatment of her primary tumor, following radical mastectomy, axillar lymphadenectomy and adjuvant radiotherapy. PDX127 was derived from a subcutaneous metastatic lesion before receiving a first-line treatment based on cisplatin and olaparib. The patient's disease achieved a partial response to the combination of agents but progressed upon switching to olaparib monotherapy. The primary tumor from patient 179 was treated with radical mastectomy and axillar lymphadenectomy, followed by adjuvant antracycline/taxane-based chemotherapy and subsequent radiotherapy. She developed a contralateral TNBC that was treated with radical mastectomy. The tumor sample for PDX implantation was obtained from a subcutaneous metastatic lesion after progression to first-line cisplatin and before olaparib treatment, whose best response was stable disease for less than 16 weeks. PDX230 was derived from a primary breast cancer, obtained after neoadjuvant antracycline/taxane-based chemotherapy, on the course of a radical

mastectomy. Following neoadjuvant therapy the patient has not presented with metastatic disease for the course of 3 years.

Supplemental References

1. Evers B et al. Selective inhibition of BRCA2-deficient mammary tumor cell growth by AZD2281 and cisplatin. *Clin. Cancer Res.* 2008;14(12):3916–3925.

2. Jaspers JE et al. Loss of 53BP1 causes PARP inhibitor resistance in Brca1-mutated mouse mammary tumors. *Cancer Discov* 2013;3(1):68–81.

3. Elstrodt F et al. BRCA1 mutation analysis of 41 human breast cancer cell lines reveals three new deleterious mutants. *Cancer Res.* 2006;66(1):41–45.

4. Tomlinson GE et al. Characterization of a breast cancer cell line derived from a germ-line BRCA1 mutation carrier. *Cancer Res.* 1998;58(15):3237–3242.

5. Jonkers J et al. Synergistic tumor suppressor activity of BRCA2 and p53 in a conditional mouse model for breast cancer. *Nat. Genet.* 2001;29(4):418–425.

6. Liu X et al. Somatic loss of BRCA1 and p53 in mice induces mammary tumors with features of human BRCA1-mutated basal-like breast cancer. *Proc. Natl. Acad. Sci. U.S.A.* 2007;104(29):12111–12116.

7. Rottenberg S et al. Selective induction of chemotherapy resistance of mammary tumors in a conditional mouse model for hereditary breast cancer. *Proc. Natl. Acad. Sci. U.S.A.* 2007;104(29):12117–12122.

8. Rottenberg S et al. High sensitivity of BRCA1-deficient mammary tumors to the PARP inhibitor AZD2281 alone and in combination with platinum drugs. *Proc. Natl. Acad. Sci. U.S.A.* 2008;105(44):17079–17084.

9. Drost R et al. BRCA1 RING function is essential for tumor suppression but dispensable for therapy resistance. *Cancer Cell* 2011;20(6):797–809.

10. Klijn C et al. Identification of cancer genes using a statistical framework for multiexperiment analysis of nondiscretized array CGH data. *Nucleic Acids Res.* 2008;36(2):e13.

11. de Ronde JJ et al. KC-SMARTR: An R package for detection of statistically significant aberrations in multi-experiment aCGH data. *BMC Res Notes* 2010;3:298.

12. Bouwman P et al. 53BP1 loss rescues BRCA1 deficiency and is associated with triple-negative and BRCA-mutated breast cancers. *Nat. Struct. Mol. Biol.* 2010;17(6):688–695.

13. Sotiropoulou PA et al. BRCA1 deficiency in skin epidermis leads to selective loss of hair follicle stem cells and their progeny. *Genes Dev.* 2013;27(1):39–51.

14. Graeser M et al. A marker of homologous recombination predicts pathologic complete response to neoadjuvant chemotherapy in primary breast cancer. *Clin. Cancer Res.* 2010;16(24):6159–6168.

15. Stap J et al. Induction of linear tracks of DNA double-strand breaks by alpha-particle irradiation of cells. *Nat. Methods* 2008;5(3):261–266.

16. Pink M, Verma N, Rettenmeier AW, Schmitz-Spanke S. CBB staining protocol with higher sensitivity and mass spectrometric compatibility. *Electrophoresis* 2010;31(4):593–598.

17. van den Berg DLC et al. An Oct4-centered protein interaction network in embryonic stem cells. *Cell Stem Cell* 2010;6(4):369–381.

18. Bouwman P et al. A high-throughput functional complementation assay for classification of BRCA1 missense variants. *Cancer Discov* 2013;3(10):1142–1155.

19. Cong L et al. Multiplex genome engineering using CRISPR/Cas systems. *Science* 2013;339(6121):819–823.

20. Brinkman EK, Chen T, Amendola M, van Steensel B. Easy quantitative assessment of genome editing by sequence trace decomposition. *Nucleic Acids Res.* 2014;42(22):e168.